

1 First of all, we appreciate the reviewer's comments. In response to the reviewer's comments, we have made
2 relevant revisions in the manuscript. Listed below are our answers and the changes made to the manuscript
3 according to the questions and suggestions given by the reviewer. Each comment of the reviewer (in black) is
4 listed and followed by our response (in blue).

5
6 **Interactive comment on "Effects of model resolution and parameterizations on the
7 simulations of clouds, precipitation, and their interactions with aerosols" by Seoung Soo Lee
8 et al.**

9 **Anonymous Referee #1**

10 Received and published: 22 June 2017

11 This manuscript is a bit of a mixed bag. I really like the analysis of the difference between the bin and bulk
12 microphysics. The analysis of resolution dependence of the clouds and cloud-aerosol interactions is not so clear,
13 as too little information is provided regarding the representation of deep convection at coarse resolution.

14 The illustrations are generally helpful, and the writing is mostly quite clear.

15 Lines 35-38. Is the comparison done at the same scale? We certainly wouldn't expect a coarse resolution
16 simulation to produce the same updraft intensity as a fine resolution simulation if they aren't compared at the
17 same scale. So I'm withholding judgement on this conclusion until I know more. Perhaps need to clarify this in
18 the text.

19 As described in Section 4.2, an identical domain for each of the Seoul and Houston cases is applied to both the
20 CSRM and GFS simulations. Stated differently, the spatial scale or the extent of the analysis area is identical
21 between the CSRM and GFS simulations, although the number of grid points in the area or the domain is
22 different between the CSRM and GFS simulations due to differences in resolutions between those simulations.
23 To clarify the point here, the following is added:

24 (LL235-238 on p12)

25 Stated differently, the spatial scale or the extent of the analysis area is identical between the CSRM simulations
26 and the GFS simulations, although the number of grid points in the area or the domain is different between the
27 CSRM simulations and the GFS simulations due to differences in resolution between those simulations.

28 Line 68. Not clear what is meant by "scale-aware schemes". Does this refer to microphysics? Please provide
29 citations.

30 Note that the traditional cumulus parameterizations are limited by the issue of scale separation (Yano, 2012).
31 Due to this limitation, the traditional cumulus parameterizations can only be used in coarse resolutions which
32 are coarser than ~ 50 km and cannot be used in fine resolutions which are finer than ~ 50 km. Nowadays, as
33 mentioned in text, many NWP models start to adopt resolutions finer than ~ 50 km and due to this, to replace
34 the traditional cumulus parameterizations, the scale-aware or scale-free schemes which can be used for any
35 resolutions whether they are coarser than ~ 50 km or not have been developed. Since the scale-aware schemes
36 are designed to replace the traditional cumulus parameterizations, the scale-aware schemes basically represent
37 sub-grid-scale convective dynamic processes (e.g., cloud-scale updrafts and downdrafts) like the traditional
38 cumulus parameterizations.

39 To clarify the point here, the following is added:

40 (LL62-65 on p3-4)

41 These scale-aware schemes, which represent sub-grid-scale dynamic processes (e.g., cloud-scale updrafts and
42 downdrafts) that are associated with cloud convection as the traditional cumulus parameterizations do, are
43 designed to be applied to the increased resolution in the NWP models.

44 We already provided citations about the scale-aware schemes in LL59-62 on p3 as follows:

45 Motivated by this, scale-aware cumulus parameterization schemes (e.g., Bogenschütz and Krueger, 2013;
46 Thayer-Calder et al., 2015; Griffin and Larson, 2016) are being implemented into these models of different
47 resolutions for better representation of clouds and precipitation.

48 Reference:

49 Yano, 2012, What is Scale Separation?: A Theoretical Reflection, obtainable at
50 http://convection.zmaw.de/fileadmin/user_upload/convection/Convection/COST_Documents/Basic_Parameterization_Concepts_and_Issues/What_is_Scale_Separation___A_Theoretical_Reflection.pdf
51

52 Line 100-102. Not clear what is meant by “RRTMG considers the effects of aerosols on the effective sizes of
53 hydrometeors”. RRTMG accounts for radiative effects of both aerosols and hydrometeors, but not the effects of
54 aerosols on hydrometeors. That is handled elsewhere, typically in the microphysics code.

55 We checked the code and found that the effective size of hydrometeors is calculated in the microphysics
56 scheme adopted and then the calculated size is transferred to the RRTMG scheme for the calculation of the
57 effects of clouds on radiation with the consideration of the effective size. To clarify this, the corresponding text
58 is revised as follows:

59 (LL101-104 on p5-6)

60 The effective sizes of hydrometeors, which vary with varying aerosol properties, are calculated in a
61 microphysics scheme that is adopted by this study and described below and the calculated sizes are transferred
62 to the RRTMG. Then, the effects of the effective sizes of hydrometeors on radiation are calculated in the
63 RRTMG.

64 Line 136. Before “less”, insert “At pressures”.

65 Done.

66 Line 141. Not clear what is meant by “cloud mass”. Is it liquid water content?

67 Cloud mass in the scheme of Moorthi et al. (2001) is represented by cloud liquid content or cloud ice content in
68 g m^{-3} , depending on temperature. Here, cloud liquid represents droplets and cloud ice represents ice crystals.
69 To clarify this, the following is added:

70 (LL156-158 on p8)

71 Here, cloud mass is represented by cloud liquid content (CLC) or cloud ice content (CIC), depending on
72 temperature, and cloud liquid (cloud ice) represents droplets (ice crystals).

73 Line 192. More description is needed here. The description of the model never discusses how turbulence or
74 convection are represented.

75 The CSRМ explicitly resolves the cloud-scale convection and thus we do not use parameterizations (e.g.,
76 cumulus parameterizations) to represent the cloud-scale convection as described in text. To clarify this better,
77 the relevant text is revised as follows:

78 (LL215-216 on p11)

79 Note that the cumulus parameterization scheme is not used in this domain where cloud-scale convection and
80 associated convective rainfall generation are assumed to be explicitly resolved.

81 To indicate how the turbulence is represented, the following is added:

82 (LL104-106 on p6)

83 The ARW model considers the sub-grid-scale turbulence by adopting 1.5-order turbulence kinetic energy
84 closure (Basu et al., 1998).

85 Lines 227-230. Much more description is needed here. Surely more was changed than resolution. The 15 km
86 and 35 km configurations must parameterize convection. How is that done?

87 Here, for those 15-km and 35-km configurations or the repeated simulations with the 15-km and 35-km
88 resolutions, we do not parameterize convection using schemes such as “cumulus parameterizations”. We just
89 want to identify the pure effects of resolutions on the simulations of clouds, precipitation, and their interactions
90 with aerosol or we simply want to identify the pure errors caused by the use of the coarse resolutions via
91 comparisons between the CSRM simulations with the 500-m or fine resolutions and the repeated simulations
92 with the 15-km and 35-km resolutions or coarse resolutions. This is why we repeat the standard CSRM runs only
93 by varying the resolutions. In case we apply the convection parameterization (which is not applied to the CSRM
94 simulations with the 500-m resolution) to the repeated simulations with the 15-km and 35-km resolutions,
95 comparisons between the CSRM simulations and repeated simulations are not able to isolate the effects of
96 resolutions due to the fact that not only resolutions but also the convection parameterization contributes to
97 differences among those simulations.

98 By only varying the resolutions among the simulations and not applying the convection parameterizations to
99 the repeated simulations with the coarse resolutions, we can say that differences between the CSRM
100 simulations (with fine resolutions) and the repeated simulations (with coarse resolutions) are the errors in the
101 simulations of clouds, precipitation, and their interactions with aerosol by taking the CSRM simulations as
102 benchmark simulations, and the varying resolutions or the coarse resolutions are the only factor that produces
103 the errors in the repeated simulations. To clarify the point here, the following is added:

104 (LL257-266 on p13-14)

105 To isolate the effects of resolution on the simulations of clouds, precipitation, and their interactions with
106 aerosols, only resolution varies among the CSRM runs at the fine resolution and the repeated runs at the coarse
107 resolutions here and these runs have an identical model setup except for resolution. For the identical setup, as
108 an example, we do not apply the convection parameterizations (e.g., cumulus parameterizations) to the
109 repeated runs, since the convection parameterizations are not applied to the CSRM runs. Hence, cloud variables
110 (e.g., the updraft speed) are not diagnosed by convection parameterizations but predicted in both the CSRM
111 runs and the repeated runs. With the identical setup except for resolution, the comparisons between the CSRM
112 simulations and the repeated simulations can isolate the pure effects of the use of coarse resolution on clouds,
113 precipitation, and their interactions with aerosol.

114 Note that the GFS simulation uses not only resolutions similar to those in the repeated simulations but also the
115 convection parameterizations or cumulus parameterizations to represent the sub-grid convection. Interestingly,
116 the GFS simulation produces results which are similar to those in the repeated simulations with the 15-km and
117 35-km resolutions and are very different from those in the CSRM simulations with the 500-m resolutions

118 despite the use of the convection parameterizations. This indicates that the use of the convection
119 parameterizations, whose purpose is to correct the errors caused by the use of coarse resolutions and then to
120 produce results similar to those in the simulations with the fine resolutions such as the CSRM simulations, does
121 not correct the errors well. This problem with the convection parameterizations is discussed in text.

122 Lines 247-248. "substantial decreases in the cloud mass at the 15- and 35-km resolutions compared to the
123 cloud mass in the simulations at the 500-m resolution". Since you refer to decreases, that suggests changes
124 with aerosol, but I'm not sure if that is what you mean. You could mean there is less cloud mass at coarse
125 resolution than at fine resolution. If you mean the latter, replace "are substantial decreases in the" with "is
126 substantially less".

127 Done.

128 Line 267. As above, change "are decreases in" to "is less".

129 Done.

130 Line 271. At fine resolution?

131 As described in Section 4.1 and in text in other sections such as that in LL 227-228 (in the old manuscript), the
132 CSRM simulations are by definition those performed with the 500-m resolution or the fine resolution. To clarify
133 this, the corresponding text is revised as follows:

134 (LL301-304 on p15-16)

135 In Figures 5 and 6, satellite-observed LWP and IWP for both cases follow reasonably well their CSRM-simulated
136 counterparts for the polluted scenario. This shows that the CSRM simulations, which are performed with the
137 500-m resolution, perform well and can thus represent benchmark simulations.

138 Line 280. More discussion is needed here. At coarser resolution the updrafts are not resolved, so aerosol
139 activation is poorly represented. If there is a cumulus parameterization, it probably lacks aerosol-aware
140 microphysics.

141 As mentioned in our response to the comment for the Lines 227-230, in the repeated simulations with the
142 coarse resolutions, we do not use cumulus parameterizations for the reasons detailed in the response to the
143 comment for the Lines 227-330. As detailed in the response, by not using cumulus parameterizations, we can
144 isolate the pure effects of the use of the coarse resolutions on clouds, precipitation, and their interactions with
145 aerosol. Here, these pure effects include the effects of updrafts not resolved by the coarse resolutions on
146 clouds, precipitation, and their interactions with aerosol via microphysical processes such as activation. As

147 detailed in our response to the comment for the Lines 227-330, these pure effects are none other than the
148 differences in results between the CSRSM simulations with the fine resolution and the repeated simulations with
149 the coarse resolutions; note that these differences represent the pure errors caused by the use of the coarse
150 resolutions (as detailed in our response to the comment for the Lines 227-330) and for example, associated
151 updrafts not resolved and poorly represented activation. These differences are compared to differences
152 between the CSRSM simulations and the GFS simulation to evaluate how the cumulus parameterization in GFS
153 works to minimize the errors. Here, the differences between the CSRSM simulations and the repeated
154 simulations with the coarse resolutions should act as a maximum extent of the errors when the cumulus
155 parameterizations to correct the errors are not used. As the differences between the CSRSM simulations and the
156 GFS simulation become closer to those between the CSRSM simulations and the repeated simulations, the
157 cumulus parameterization used in the GFS simulation is considered to be working worse. Stated differently, if
158 there are no differences in results between the CSRSM simulations and the GFS simulation, the cumulus
159 parameterization in the GFS simulation is considered to work perfect. Here, as mentioned in text, the CSRSM
160 simulations act as benchmark simulations and this is proven by comparisons between the CSRSM simulations
161 and observations.

162 In summary, here, the pure errors include those caused by updrafts not resolved and poorly represented
163 activation as exemplified by the reviewer here and we quantify these errors via the comparisons between
164 simulations as described above and based on quantification, we provide a guideline by which the
165 parameterizations in GFS can be developed in an efficient way; see our discussion related to this in the last five
166 paragraphs of “summary and discussion”

167 Lines 283-285. If the GFS model lacks aerosol-aware physics then there would be little sensitivity to aerosol. The
168 description of the GFS does not indicate any dependence on aerosol.

169 It is true that there is no “aerosol-aware physics” in the current GFS. However, in the text pointed out here, it is
170 meant that even though aerosol-aware physics is implemented into GFS, it is likely that GFS shows the weak
171 sensitivity (to increasing aerosol concentration) as shown in the ARW simulations at the coarse resolution.

172 The cumulus parameterization in the current GFS is not able to correct errors in variables such as updrafts to
173 result in the similarity between the GFS simulation and the ARW simulations at the coarse resolutions. The ARW
174 simulations which are equipped with the aerosol-aware physics and at the coarse resolutions demonstrate that
175 when those errors are not corrected or updrafts are underestimated (as compared to the CSRSM simulations),
176 even the presence of “aerosol-aware physics” does not prevent the weak sensitivity to increasing aerosol
177 concentrations. Hence, the current GFS, which does not correct errors in updrafts well or underestimates
178 updrafts as discussed in “summary and discussion”, is likely to show the weak sensitivity even though “aerosol-
179 aware physics” is implemented into GFS.

180 To clarify the point here, the following is added:

181 (LL363-374 on p19)

182 Taking the sensitivity of updraft mass fluxes to increasing aerosol concentrations in the CSRM simulations as the
183 benchmark sensitivity, the GFS simulations likely also underestimate the sensitivity, considering the similarity in
184 results between the ARW simulations at the 15- and 35-km resolutions and the GFS simulations. Since the
185 current GFS model does not consider pathways through which increasing aerosol concentrations interact with
186 updraft mass fluxes, this probable underestimation of the sensitivity is even more likely. Note that the ARW
187 simulations which are at the 15- and 35-km resolutions and underestimate updrafts themselves, even with the
188 consideration of those pathways, result in the much weaker sensitivity at the coarse resolutions as compared to
189 that in the CSRM simulations. Hence, even though those pathways are implemented into the GFS model, the
190 underestimated updrafts in the GFS simulations are likely to result in the weak sensitivity, unless the cumulus
191 parameterization which represents updrafts in the GFS model is further developed to prevent the
192 underestimation of updrafts.

193

194 Line 291. Need discussion of how convection is represented in ARW at different resolutions. I assume the
195 updraft mass flux in the course simulations is diagnosed from the convection scheme.

196 The convection scheme such as the cumulus parameterization is not used in the ARW simulations at all of the
197 different resolutions due to the reasons which are elaborated in our response to the comment for the Lines
198 227-230. The discussion of how convection is presented in the ARW simulations at different resolutions is given
199 as follows:

200 (LL257-266 on p13-14)

201 To isolate the effects of resolution on the simulations of clouds, precipitation, and their interactions with
202 aerosols, only resolution varies among the CSRM runs at the fine resolution and the repeated runs at the coarse
203 resolutions here and these runs have an identical model setup except for resolution. For the identical setup, as
204 an example, we do not apply the convection parameterizations (e.g., cumulus parameterizations) to the
205 repeated runs, since the convection parameterizations are not applied to the CSRM runs. Hence, cloud variables
206 (e.g., the updraft speed) are not diagnosed by convection parameterizations but predicted in both the CSRM
207 runs and the repeated runs. With the identical setup except for resolution, the comparisons between the CSRM
208 simulations and the repeated simulations can isolate the pure effects of the use of coarse resolution on clouds,
209 precipitation, and their interactions with aerosol.

- 210 Lines 307-310. The difference could be due to poor parameterization of convection in both models. More
211 information is needed.
- 212 [See our responses to the comments on Line 280 and Lines 283-285.](#)
- 213 Lines 311-312. Even if the GFS simulated the updraft mass flux correctly, it would likely still underestimate the
214 sensitivity to the aerosol because it lacks the physics that drives the sensitivity.
- 215 [See our responses to the comment on Lines 283-285. Based on them and the fact that the CSRMs simulations act](#)
216 [as benchmark simulations that predict updrafts correctly and show the benchmark sensitivity to the aerosol, it](#)
217 [is believed that in case the GFS simulation predicts the updraft mass flux correctly and is equipped with](#)
218 [“aerosol-aware physics” like the CSRMs simulations, the GFS simulation is likely to produce a correct sensitivity.](#)
- 219 Line 313. How do you get updraft speed from updraft mass flux? Cumulus parameterizations produce mass flux,
220 but additional assumptions are needed to diagnose updraft speed. More detail is needed here.
- 221 [In the ARW simulations at any resolutions, as explained in our responses above, cumulus parameterizations are](#)
222 [not used. Instead, in those ARW simulations, the updraft speed itself is predicted by the ARW model. Then the](#)
223 [updraft mass flux is obtained simply by multiplying the updraft speed with air density. To clarify the point here,](#)
224 [the following is added:](#)
- 225 [\(LL262-264 on p13-14\)](#)
- 226 [Hence, cloud variables \(e.g., the updraft speed\) are not diagnosed by convection parameterizations but](#)
227 [predicted in both the CSRMs runs and the repeated runs.](#)
- 228 [\(LL324-325 on p17\)](#)
- 229 [Updraft mass fluxes are obtained by multiplying the predicted updraft speed by air density.](#)
- 230 Lines 323-339. Do the convection schemes in the models have any physics that would cause the updrafts to
231 depend on aerosol?
- 232 [As elaborated in our responses above, the convection schemes are not used in the ARW simulations at any](#)
233 [resolutions in this paper. Instead, based on results from those simulations, the discussion about the convection](#)
234 [schemes with the dependence on aerosol is given in “summary and discussion”; see the last paragraph in the](#)
235 [paper for the discussion.](#)
- 236 Section 5.2. Excellent work and presentation!

237 Lines 468-473. Some discussion of the microphysics in the convection schemes used in the coarse resolution
238 simulations would be helpful.

239 As elaborated in our responses above, the convection schemes are not used in the ARW simulations at any
240 resolutions in this paper.

241 Lines 519-520. It should be noted here that in saturation adjustment schemes the condensed water does not
242 depend on updraft velocity. And the coarse resolution models lack dependence of cumulus microphysics on
243 supersaturation.

244 We believe that saturation adjustment calculates the amount of water vapor that should be condensed based
245 on the predicted or diagnosed updrafts and the associated level of saturation. Even in saturation adjustment,
246 stronger updrafts produce a lower level of saturation for a given amount of water vapor to result in more
247 condensed water vapor that affects associated microphysical processes, as in schemes that predict
248 supersaturation. However, in saturation adjustment, the entire amount of water vapor that is determined to be
249 condensed is removed from the atmosphere within one time step, which is different from those schemes that
250 predict supersaturation or the supersaturation prediction; Tao et al. (1989) is one of classic papers on
251 saturation adjustment and see this paper for the details of saturation adjustment. Hence, in saturation
252 adjustment, condensed water depends on updrafts or updraft speed. Stated differently, even in saturation
253 adjustment, the underestimation of the updraft intensity leads to the underestimation of condensed water and
254 thus cloud mass. Based on this, whether the NWP models adopt saturation adjustment (and its impacts on
255 microphysics) or supersaturation prediction (and its impacts on microphysics), the use of coarse resolutions in
256 the NWP models, which results in the underestimation of updrafts, induces the underestimation of condensed
257 water and cloud mass. As detailed in our responses to some of the comments above, whether the NWP models
258 adopt “aerosol-aware physics (that considers the effect of updrafts and supersaturation (or the saturation level)
259 on cumulus microphysics and aerosol impacts on the effect)” as phrased by the reviewer above, the NWP
260 models are likely to underestimate cloud variables (e.g., updrafts, condensed water and cloud mass) and the
261 sensitivity of cloud variables to increasing aerosol concentrations based on the ARW simulations.

262 Text pointed out here is revised as follows to remove impression that the statement in this text is only
263 applicable to the supersaturation prediction but not the saturation adjustment:

264 (LL577-579 on p29)

265 This study shows that the use of coarse resolution can cause an underestimation of the updraft intensity and
266 thus condensation and deposition, which leads to an underestimation of the cloud mass.

267 Reference:

268 Tao, W. K., J. Simpson, and M. McCumber, 1989, An ice-water saturation adjustment, *J. Appl. Meteor.*, 117,
269 231-235.

270 Lines 555-570. This is great discussion. Perhaps note that global models designed to represent cloud-aerosol
271 interactions do use a subgrid updraft velocity for activation in stratiform clouds, so they would exhibit less
272 resolution dependence of clouds than the ARW model. See, e.g, Ghan et al. JGR 1997.

273 As detailed in our discussion (LL540-554 in the old manuscript), although the GFS model is coupled to the sub-
274 grid parameterizations or the convection scheme such as cumulus parameterizations that diagnose the subgrid
275 variables such as the subgrid updraft speed, the GFS model produces the results similar to those in the ARW
276 simulations at the coarse resolution. As detailed in our discussion (LL540-554 in the old manuscript), this means
277 that the diagnosis of the subgrid variables (by the convection scheme) and the calculation of their impacts on
278 microphysical processes such as activation do not work well in the GFS model. Associated with this, as detailed
279 in our responses to some of the reviewer's comments above, although "aerosol-aware physics" as phrased by
280 the reviewer here is implemented into GFS, GFS is likely to show the weak sensitivity (to increasing aerosol
281 concentration) as shown in the ARW simulations at the coarse resolution. Stated differently, the GFS model
282 (representing global models) which considers cloud-aerosol interactions is likely to produce the weak
283 sensitivity or the underestimation of the sensitivity, unless the convection scheme is improved to remove the
284 errors that are caused by the use of the coarse resolution and the subsequent incorrect diagnosis of the subgrid
285 variables. This discussion about the GFS model (representing global models) is all about the GFS model at the
286 coarse resolution. In this study, we assume that in case GFS model adopts the resolution as fine as in the CSR
287 simulations, the GFS model does not have to use the convective schemes as in the CSR simulations, since
288 cloud variables such as updrafts are considered to be explicitly resolved at the fine resolution. Considering that
289 the dependence of model results on microphysics parameterizations is very small as compared to that on
290 resolutions as discussed in Section 5.3, we assume that the GFS model (representing the global models)
291 produce results (including the sensitivity) similar to those in the CSR as long as the GFS model uses the
292 resolution as fine as in the CSR and thus explicitly resolves updrafts as in the CSR, although there can be
293 differences in physics parameterizations between the GFS and the CSR. Based on this assumption and the fact
294 that at the coarse resolution, results are similar between the GFS model and the ARW model, we believe that
295 the variation of results (including the sensitivity) among the ARW simulations with a transition from a fine
296 resolution to a coarse resolution is likely to be similar to that variation among the GFS simulations with that
297 transition.

298

299

300

301 First of all, we appreciate the reviewer's comments. In response to the reviewer's comments, we have made relevant revisions
302 in the manuscript. Listed below are our answers and the changes made to the manuscript according to the questions and suggestions
303 given by the reviewer. Each comment of the reviewer (in black) is listed and followed by our response (in blue).

304
305 **Interactive comment on “Effects of model resolution and parameterizations on**
306 **the simulations of clouds, precipitation, and their interactions with aerosols” by**
307 **Seoung Soo Lee et al.**

308 **Anonymous Referee #2**

309
310 Received and published: 29 June 2017

311
312 This paper nicely demonstrates the role of spatial resolution and microphysics in determining differences between a model with
313 high resolution and bin representation of microphysics compared to low resolution and bulk representation of microphysics. It
314 should be published after clarification of the following and/or improvement in wording.

315
316 Many places use “resolutions” where I would have thought “resolution” was best English usages.

317
318 We went through text and replaced “resolutions” with “resolution” when needed.

319
320 Line 71: Change “These” to This

321
322 Done.

323
324 Line 136: change “less than” to “above”

325
326 Following the other reviewer's comment, “less than” is replaced with “At pressures less than”

327
328 Lines 118 – 126: this cannot be the full description of ammonium sulfate sources and sinks, since it only describes the interaction
329 of aerosol with clouds. What about nucleation from the gas phase production of sulfate? How is gas phase sulfate produced? Do
330 you represent condensation onto existing aerosols? What about dry deposition loss?

331
332 In this study, we focus on interactions among aerosol, clouds, and precipitation but not on aerosol physics and chemistry. Stated
333 differently, this study aims to examine errors and mechanisms that govern those errors in the simulations of aerosol-cloud-
334 precipitation interactions themselves by the NWP models as stated in “introduction”. Thus, the examination of errors and
335 associated mechanisms in the simulations of aerosol physics and chemistry by the NWP models is out of scope of this study. Based
336 on this, we do not explicitly simulate aerosol physics and chemistry and we prescribe aerosol physical and chemical properties. To
337 clarify the points here, the following is added:

338
339 (LL123-130 on p7)

340
341 As stated in introduction, this study focuses on the uncertainties or errors in the simulations of clouds, precipitation, and CAPI
342 themselves. This means that the examination of the uncertainties in the simulations of aerosol physics and chemistry is out of scope
343 of this study. Hence, in this study, instead of simulating aerosol physics and chemistry explicitly, initial aerosol physical and
344 chemical properties (i.e., aerosol chemical composition and size distribution) are prescribed. Then, aerosol size distribution (or
345 aerosol number concentration in each size bin) evolves only through cloud processes but not through aerosol physical and chemical
346 processes. During the evolution, the prescribed aerosol composition is assumed not to vary.

347
348 Fig 1a,b: please increase size of rectangle, similar to 1c, d.

301
302
303
304
305
306
307
308
309
310
311
312
313
314
315
316
317
318
319
320
321
322
323
324
325
326
327
328
329
330
331
332
333
334
335
336
337
338
339
340
341
342
343
344
345
346
347
348
349

350 Done.

351
352 Model set up: What is used for boundary conditions for the CSRMs? How do these boundary conditions compare to the incoming
353 air in the GFS simulations?

354
355 For the ARW simulations (including the CSRMs simulations), we use open lateral boundary conditions and hence, the synoptic
356 conditions are advected into and out of the domain by air through the boundary of the domain. This emulates the situation in the
357 GFS simulations where the synoptic conditions are advected into and out of an area (corresponding to the domain in the ARW
358 simulations) by air through the border between the area and places outside the area. In the ARW simulations, the synoptic
359 conditions are derived from the National Centers for Environmental Prediction GFS final (FNL) analysis. The FNL analysis is
360 based on environmental conditions that are produced by GFS and thus there are basically no differences in the synoptic conditions
361 between those advected into and out of the domain in the ARW simulations by air and those advected into and out of the area
362 (corresponding to the domain in the ARW simulations) in the GFS simulations by air.

363
364 In summary, the domain in the ARW simulations and the area (corresponding to the domain in the ARW simulations) in the GFS
365 simulations experience an identical synoptic condition. The advection of the synoptic condition into and out of the domain by air in
366 the ARW simulations is through the boundary of the domain, which is enabled by the use of the open boundary conditions and
367 emulates the advection of the synoptic condition into and out of the area in the GFS simulations through the border between the
368 area and places outside the area.

369
370 To clarify the point here, the following is added:

371
372 (LL198-205 on p10-11)

373
374 Initial and boundary conditions, which represent the synoptic features, for the control run are derived from the National Centers for
375 Environmental Prediction GFS final (FNL) analysis. Since the FNL analysis is based on environmental conditions that are
376 produced by the GFS model and thus for each of the cases, there are basically no differences in the synoptic condition between the
377 CSRMs simulations and the GFS simulations that are described in the following Section 4.2. The open lateral boundary condition is
378 adopted in the control run. This enables the advection of the synoptic condition into and out of a domain in the CSRMs simulations
379 to occur through the boundary of the domain, which emulates the advection in the GFS simulations.

380
381 Line 294: what are the deposition rates shown in Fig 9? This is not surface deposition, since the units are wrong.

382
383 In this paper, condensation, evaporation, and deposition occur on the surface of hydrometeors. Condensation and evaporation occur
384 on the surface of drops, while deposition occurs on the surface of solid hydrometeors such as ice crystals; deposition is, by
385 definition in microphysics, the diffusion of water vapor onto solid hydrometeors such as ice crystals in clouds. In this paper,
386 condensation rate and evaporation rate are defined as the rates of changes in drop mass (or liquid mass) in a unit volume of air and
387 for a unit time due to condensation and evaporation, respectively, following the conventional definition of condensation and
388 evaporation rates in cloud community. Deposition rate is defined as the rate of changes in the mass of solid hydrometeors (or ice
389 mass) in a unit volume of air and for a unit time due to deposition, following the conventional definition of deposition rate in cloud
390 community. To clarify this, the following is added:

391
392 (LL331-333 on p17)

393
394 Here, condensation and deposition rates are defined as the rates of changes in liquid mass and ice mass in a unit volume of air and
395 for a unit time due to condensation and deposition on the surface of hydrometeors, respectively.

396
397 (LL414-416 on p21)

398
399 Here, evaporation rate is defined as the rate of changes in liquid mass in a unit volume of air and for a unit time due to evaporation
400 on the surface of hydrometeors.

401 Line 298-300: why do updraft mass fluxes increase with higher aerosol?
402

403
404 As stated in text (LL331-335) in the old manuscript, aerosol-induced invigoration of convection through aerosol-induced increases
405 in freezing or aerosol-induced intensification of gust fronts is the main mechanism behind aerosol-induced increases in updraft
406 mass fluxes or the intensity of updrafts. To provide more detailed information on aerosol-induced invigoration of convection, the
407 following is added:

408
409 (LL336-349 on p17-18)

410
411 Increasing aerosol concentrations alter cloud microphysical properties such as drop size and autoconversion. Aerosol-induced
412 changes in autoconversion in turn increase cloud-liquid mass as a source of evaporation and freezing. Numerous studies (e.g.,
413 Khain et al., 2005; Seifert and Beheng, 2006; Tao et al., 2007, 2012; van den Heever and Cotton, 2007; Storer et al., 2010; Lee et
414 al., 2013, 2017) have shown that aerosol-induced increases in cloud-liquid mass and associated increases in freezing of cloud liquid
415 enhance the freezing-related latent heating and thus parcel buoyancy, and this invigorates convection or increases updraft mass
416 fluxes. Those studies have also shown that the aerosol-induced increases in cloud-liquid mass and associated increases in the
417 evaporation of cloud liquid enhance the evaporation-related latent cooling and thus negative buoyancy. This intensifies downdrafts
418 and after reaching the surface, the intensified downdrafts spread out toward the surrounding warm air to form intensified gust
419 fronts and then, to uplift the warm air more strongly. More strongly uplifted warm air leads to invigorated convection or increased
420 updraft mass fluxes. These freezing- and evaporation-related invigoration mechanisms are operative to induce the aerosol-induced
421 enhancement of updraft mass fluxes, condensation, and deposition in this study.

422
423 Line 526: what are “high-level” updrafts? At high altitude? Similar comment for lowlevel updrafts. You did not discuss this in the
424 paper. (also only updraft mass flux is in figures).
425

426 Discussion in the paragraph related to this comment is based on Figure 7 that shows the vertical distributions of the time- and
427 domain-averaged updraft mass fluxes in the ARW simulations. Just want to note that updraft mass fluxes are obtained by
428 multiplying the predicted updraft speed (or updrafts) with air density. Since there are negligible differences in air density among
429 simulations at different resolutions, differences in updraft mass fluxes among those simulations are mostly caused by differences in
430 the updraft speed or updrafts. This means that the qualitative nature of discussion about the differences in updraft mass fluxes
431 among simulations is not different from that of discussion about the differences in the updraft speed or updrafts. Hence, discussion
432 in paragraphs using the word “updrafts” can be replaced with discussion using the word “updraft mass fluxes”. In the paragraph,
433 high-level and low-level simply mean high-value and low-value, respectively.
434

435 To clarify our points here, the following is added:

436
437 (LL324-329 on p17)

438
439 Updraft mass fluxes are obtained by multiplying the predicted updraft speed by air density. Since there are negligible differences in
440 air density among the ARW simulations, most of differences in updraft mass fluxes among the simulations are caused by
441 differences in the updraft speed or updrafts. Those differences in air density are in general ~ two orders of magnitude smaller than
442 those in the updraft speed or updrafts.
443

444 Based on our points here, the corresponding text is revised as follows:

445
446 (LL585-588 on p30)

447
448 When they are resolved with the use of high-resolution models, there are high-value averaged updrafts and associated variables,
449 and their strong sensitivity but when they are not resolved in low-resolution models, there are low-value averaged updrafts and
450 associated variables, and their weak sensitivity.
451

**Effects of model resolution and parameterizations on the simulations of clouds, precipitation,
and their interactions with aerosols**

Seoung Soo Lee¹, Zhanqing Li¹, Yuwei Zhang¹, Hyelim Yoo², Seungbum Kim³, Byung-Gon Kim⁴,
Yong-Sang Choi⁵

¹Earth System Science Interdisciplinary Center, University of Maryland, College Park, Maryland

²Earth Resources Technology, Inc., National Oceanic and Atmospheric Administration, College Park,
Maryland

³Weather Impact Forecasts Team, Korea Meteorological Administration, Seoul, South Korea

⁴Department of Atmospheric Environmental Sciences, Gangneung-Wonju National University,
Gangneung, Gang-Won do, South Korea

⁵Department of Environmental Science and Engineering, Ewha Womans University, Seoul, South
Korea

Corresponding author: Seoung Soo Lee

Office: (303) 497-6615

Cell: (609) 375-6685

Fax: (303) 497-5318

E-mail: cumulss@gmail.com, slee1247@umd.edu

Deleted:

Formatted: Superscript

Formatted: Superscript

Formatted: Superscript

Formatted: Superscript

Deleted: ¶

Deleted: ¶

¶
¶
¶
¶
¶
¶
¶

Abstract

This study investigates the effects of model resolution and microphysics parameterizations on the uncertainties or errors in the simulations of clouds, precipitation, and their interactions with aerosols using the Global Forecast System (GFS) model as one of the representative numerical weather prediction (NWP) models. For this investigation, we used the GFS model results and compare them with those from the cloud-system resolving model (CSRМ) simulations as benchmark simulations that adopt a high resolution and full-fledged microphysical processes. These simulations were evaluated against observations and this evaluation demonstrated that the CSRМ simulations can function as benchmark simulations. Substantially lower updrafts and associated cloud variables (e.g., cloud mass and condensation) were simulated by the GFS model compared to those simulated by the CSRМ. This is mainly due to coarse resolution in the GFS model. This indicates that the parameterizations that represent sub-grid processes in the GFS model do not work well and thus need to be improved. Results here also indicate that the use of coarse resolution in the GFS model lowers the sensitivity of updrafts and cloud variables to increasing aerosol concentrations compared to the CSRМ simulations. The parameterization of the saturation process plays an important role in the sensitivity of cloud variables to aerosol concentrations while the parameterization of the sedimentation process has a substantial impact on how cloud variables are distributed vertically. The variation in cloud variables with resolution is much greater and contributes to the discrepancy between the GFS and CSRМ simulations to a much greater degree than what happens with varying microphysics parameterizations.

Deleted: s

Deleted: the

Deleted: s

Deleted: the

1. Introduction

The treatment of clouds and precipitation and their interactions with aerosols in the NWP models is likely a major source of errors in the simulations of the water and energy cycles (Sundqvist et al., 1989; Randall et al., 2006; Seifert et al., 2012). The NWP community has recognized that the accurate representation of clouds, precipitation, and cloud-aerosol-precipitation interactions (CAPI) is important for the improvement of the NWP models and thus, some of these models have started to improve the representation by considering CAPI (Morcrette et al., 2011; Sudhakar et al., 2016).

CAPI may not have a substantial impact on the total precipitation amount but they do affect the temporal and spatial variabilities of precipitation (Li et al., 2011; van den Heever et al., 2011; Seifert et al., 2012; Lee and Feingold, 2013; Fan et al., 2013; Lee et al., 2014), whose importance increases as the temporal/spatial scales of forecast decrease. The distribution of extreme precipitation events such as droughts and floods, closely linked to the spatiotemporal variability, has important social and economic implications.

In recent years, resolution in the NWP models has increased to the point that the traditional cumulus parameterization schemes may no longer work properly. Motivated by this, scale-aware cumulus parameterization schemes (e.g., Bogenschutz and Krueger, 2013; Thayer-Calder et al., 2015; Griffin and Larson, 2016) are being implemented into these models of different resolutions for better representation of clouds and precipitation. These scale-aware schemes, which represent sub-grid-scale dynamic processes (e.g., cloud-scale updrafts and downdrafts) that are associated with cloud convection

Deleted: s

Deleted: ve

531 as the traditional cumulus parameterizations do, are designed to be applied to the increased resolution
 532 in the NWP models.

533 The uncertainties or the errors in the simulations of clouds, precipitation, and CAPI in the NWP
 534 models may be incurred both from microphysics parameterizations and from model resolution. The
 535 implementation of the cloud microphysics such as the two-moment (e.g. Morrison and Gettelman, 2008;
 536 Morrison et al., 2009) and scale-aware schemes are intended to reduce these uncertainties. It is
 537 important to first understand and quantify the uncertainties associated with the two-moment scheme and
 538 how model resolution creates the uncertainties, as well as the relative significance between the
 539 uncertainties associated with the two-moment scheme and those created by resolution. This
 540 understanding and quantification can provide us with a guideline on how to represent microphysics in
 541 the two-moment schemes and sub-grid processes in the scale-aware schemes for the efficient reduction
 542 of the uncertainties in the NWP models. Note that the representation of sub-grid processes requires
 543 information on the contribution of resolution to the uncertainties and, in this study, we focus on the two-
 544 moment scheme developed by Morrison and Gettelman (2008) and Morrison et al. (2009), which is
 545 referred to as the MG scheme, henceforth.

546 Fan et al. (2012) and Khain et al. (2015) have shown that the parameterizations of three key
 547 microphysical processes (i.e., saturation, collection, and sedimentation) in microphysical schemes act as
 548 a main source of errors in the simulation of clouds, precipitation, and CAPI. We try to identify and
 549 quantify the errors or the uncertainties through comparisons between simulations with
 550 parameterizations of the three key processes in the MG scheme and the CSRMs simulations with full-

Deleted: s

Deleted: s

Deleted: the

Deleted: s

Deleted: ese

556 fledged microphysical processes. Regarding the understanding of the uncertainties arising from the
557 choice of resolution, we also perform comparisons between the high-resolution CSRМ simulations and
558 the low-resolution simulations, and do additional comparisons with the GFS simulations. This helps
559 gain an understanding of how the microphysical representation and coarse resolution in the GFS model
560 (as compared to those in the CSRМ) contribute to the uncertainties in the GFS simulations of clouds
561 and precipitation by accounting for CAPI. Here, the CSRМ simulations act as benchmark simulations
562 by representing microphysical processes with high-level sophistication and by resolving cloud-scale
563 physical and dynamic processes with a high resolution.

Deleted: s

565 2. Models

567 2.1 The CSRМ

569 The Advanced Research Weather Research and Forecasting (ARW) model, a non-hydrostatic
570 compressible model, is the CSRМ selected for use in this study. A fifth-order monotonic advection
571 scheme is used for the advection of cloud variables (Wang et al., 2009). The ARW model considers
572 radiation processes by adopting the Rapid Radiation Transfer Model for General Circulation Models
573 (RRTMG) (Fouquart and Bonnel, 1980; Mlawer et al., 1997). The effective sizes of hydrometeors,
574 which vary with varying aerosol properties, are calculated in a microphysics scheme that is adopted by
575 this study and described below and the calculated sizes are transferred to the RRTMG. Then, the effects

Deleted: The RRTMG considers

578 of the effective sizes of hydrometeors on radiation are calculated in the RRTMG. The ARW model
579 considers the sub-grid-scale turbulence by adopting 1.5-order turbulence kinetic energy closure (Basu et
580 al., 1998).

Deleted: aerosols on

Deleted: and the associated changes in

581 For an assessment of the uncertainties in the MG scheme, which is a type of a bulk scheme, we
582 need to use microphysics schemes that are much more sophisticated than the MG scheme. Through
583 extensive comparisons between various types of bin schemes and bulk schemes, Fan et al. (2012) and
584 Khain et al. (2015) have concluded that the use of bin schemes or bin-bulk schemes is desirable for
585 reasonable simulations of clouds, precipitation, and their interactions with aerosols. This is because
586 these schemes do not use a saturation adjustment, a mass-weight mean terminal velocity, or constant
587 collection efficiencies that have been used in bulk schemes. Instead, bin schemes use predicted
588 supersaturation levels, and terminal velocities and collection efficiencies that vary with the sizes of
589 hydrometeors. Based on the work by Fan et al. (2012) and Khain et al. (2015), this study considers bin
590 schemes to be a full-fledged microphysics schemes against which the uncertainties in the MG scheme
591 can be assessed. Hence, a bin scheme is adopted in the CSRM used here.

592 The bin scheme adopted by the CSRM is based on the Hebrew University Cloud Model described
593 by Khain and Lynn (2009). The bin scheme solves a system of kinetic equations for the size distribution
594 functions of water drops, ice crystals (plate, columnar and branch types), snow aggregates, graupel and
595 hail, as well as cloud condensation nuclei. Each size distribution is represented by 33 mass-doubling
596 bins, i.e., the mass of a particle m_k in the k^{th} bin is $m_k = 2m_{k-1}$.

599 As stated in introduction, this study focuses on the uncertainties or errors in the simulations of
600 clouds, precipitation, and CAPI themselves. This means that the examination of the uncertainties in the
601 simulations of aerosol physics and chemistry is out of scope of this study. Hence, in this study, instead
602 of simulating aerosol physics and chemistry explicitly, initial aerosol physical and chemical properties
603 (i.e., aerosol chemical composition and size distribution) are prescribed. Then, aerosol size distribution
604 (or aerosol number concentration in each size bin) evolves only through cloud processes (as described
605 below) but not through aerosol physical and chemical processes. During the evolution, the prescribed
606 aerosol composition is assumed not to vary.

607 In this study, it is assumed that aerosol particles are composed of ammonium sulfate. The aerosol
608 size distribution evolves, prognostically with sinks and sources, which include advection, droplet
609 nucleation, and aerosol regeneration from droplet evaporation (Fan et al., 2009). Aerosol activation is
610 calculated according to the Köhler theory, i.e., aerosol particles with radii exceeding the critical value at
611 a grid point are activated to become droplets based on predicted supersaturation, and the corresponding
612 bins of the aerosol spectra are emptied. After activation, the aerosol mass is transported within
613 hydrometeors by collision-coalescence and removed from the atmosphere once hydrometeors that
614 contain aerosols reach the surface. Aerosol particles return to the atmosphere upon evaporation or the
615 sublimation of hydrometeors that contain them. ▲

Deleted: I

Deleted: is calculated

Formatted: Font: (Asian) Times New Roman

617 2.2 The GFS model

618

621 The GFS model is a global NWP model that is run by the National Oceanic and Atmospheric
 622 Administration (NOAA). The GFS model has 64 vertical sigma-pressure hybrid layers and a T382 (~ 35
 623 km) horizontal resolution. Output fields for a forecast generated at 3-hour intervals (i.e. at 03, 06, 09, 12,
 624 15, 18, 21, 24 universal coordinated time, or Z), starting from the control time of 00Z, are used for this
 625 study.

626 The GFS model posts parameters for 21 vertically different layers. From the surface (1000 hPa) to
 627 the 900-hPa level, the vertical resolution is 25 hPa. ~~At pressures less than 900 hPa, there are 16 levels at~~
 628 a 50-hPa resolution up to 100 hPa. The cloud phase is determined by the mean temperature (T_c) of a
 629 cloud layer which is defined as the average of temperatures at the top and bottom of a cloud layer. If T_c
 630 is less than 258.16 K, the cloud layer is an ice cloud; otherwise, it is a water cloud.

631 A prognostic condensate scheme by Moorthi et al. (2001) has been used to parameterize clouds in
 632 the GFS model. In this scheme, cloud mass, one of the representative cloud variables, evolves by
 633 considering the cloud-mass advection, diffusion and conversion to precipitation, and the diagnosed sub-
 634 grid and grid-scale ~~phase-transition processes (e.g., condensation and evaporation). Here, cloud mass is~~
 635 ~~represented by cloud liquid content (CLC) or cloud ice content (CIC), depending on temperature, and~~
 636 ~~cloud liquid (cloud ice) represents droplets (ice crystals).~~ The grid-scale ~~phase-transition processes,~~ are
 637 calculated based on Sundqvist et al. (1989) and Zhao and Carr (1997), while the sub-grid ~~transition~~
 638 ~~processes,~~ are calculated based on a cumulus parameterization that adopts the mass-flux approach. This
 639 cumulus parameterization was developed by Moorthi et al. (2001) based on a simplified Arakawa-
 640 Schubert scheme (Pan and Wu, 1995).

Deleted: L

Deleted: condensation and evaporation

Deleted: .

Deleted: condensation and evaporation

Deleted: condensation and evaporation

646

647 **3. The cases**

648

649 **3.1 The Seoul case**

650

651 A mesoscale convective system (MCS) was observed over Seoul, Korea (37.57°N, 126.97°E; 0900 local
652 solar time (LST) 26 July 2011–0900 LST 27 July 2011). This case, referred to as the Seoul case,
653 involved heavy rainfall with a maximum precipitation rate of $\sim 150 \text{ mm h}^{-1}$. This heavy rainfall caused
654 flash floods and landslides on a mountain at the southern flank of the city, leading to the deaths of 60
655 people.

656 At 0900 LST July 26th 2011, favorable synoptic-scale features for the development of heavy
657 rainfall over Seoul were observed. The western Pacific subtropical high (WPSH) was located over the
658 southeast of Korea and Japan, and there was a low-pressure trough over north China (Figure 1a). Low-
659 level jets between the flank of the WPSH and the low-pressure system brought warm, moist air from the
660 Yellow Sea to the Korean Peninsula (Figure 1b). Transport of warm and moist air by the southwesterly
661 low-level jet is an important condition for the development of heavy rainfall events over Seoul (Hwang
662 and Lee, 1993; Sun and Lee, 2002).

663

664 **3.2 The Houston case**

665

666 An MCS was observed over Houston, Texas (29.42°N, 94.45°W; 0700 LST 18 July 2013–0400 LST
667 19 July 2013). The Houston case involved moderate rainfall with a maximum precipitation rate of ~50
668 mm h⁻¹.

669 At 0500 LST, two hours before the initiation of convection, the low-level wind in and around
670 Houston was southerly (Figure 1c), favoring the transport of water vapor from the Gulf of Mexico to
671 the Houston area. Associated with this, the environmental convective available potential energy (CAPE)
672 (Figure 1d) in and around Houston along the coastline was high (as represented by red areas in Figure
673 1d). The high CAPE provided a favorable condition for the development of the MCS.

674

675 **4. Simulations**

676

677 **4.1 The CSRM simulations**

678

679 Using the ARW model and its bin scheme, a three-dimensional CSRM simulation of the observed MCS
680 was performed over the MCS period for each of the cases.

681 Initial and boundary conditions, which represent the synoptic features, for the control run are
682 derived from the National Centers for Environmental Prediction GFS final (FNL) analysis. Since the
683 FNL analysis is based on environmental conditions that are produced by the GFS model and thus for
684 each of the cases, there are basically no differences in the synoptic condition between the CSRM
685 simulations and the GFS simulations that are described in the following Section 4.2. The open lateral

686 boundary condition is adopted in the control run. This enables the advection of the synoptic condition
 687 into and out of a domain in the CSRM simulations to occur through the boundary of the domain, which
 688 emulates the advection in the GFS simulations. All experiments employ a prognostic surface skin
 689 temperature scheme (Zeng and Beljaars, 2005) and a revised roughness length formulation (Donelan et
 690 al., 2004).

691 The control run for each of the cases consists of a domain with a Lambert conformal map
 692 projection. The domain is marked by the rectangle for the Seoul case in Figure 2a and the domain for
 693 the Houston case is shown in Figure 2b. While the control run for the Seoul case is referred to as “the
 694 control-Seoul run”, the control run for the Houston case is referred to as “the control-Houston run”,
 695 henceforth. The domain for the Seoul (Houston) case covers the Seoul (Houston) area and to resolve
 696 cloud-scale processes, a 500-m horizontal resolution is applied to the domain. The domain has 41
 697 vertical layers with the vertical resolution ranging from 70 m near the surface to 800 m at the model top
 698 (~50 hPa). Note that the cumulus parameterization scheme is not used in this domain where cloud-scale
 699 convection and associated convective rainfall generation are, assumed to be explicitly resolved. Based
 700 on observations, the aerosol concentration at the surface at the first time step is set at 5500 (1500) cm^{-3}
 701 for the Seoul (Houston) case. Above the top of the planetary boundary layer (PBL) around 2 km, the
 702 aerosol concentration reduces exponentially.

703 To examine and isolate CAPI, i.e., the effect of increasing the loading of aerosols on clouds and
 704 precipitation, the control run is repeated with the aerosol concentration at the first time step reduced by
 705 a factor of 10. This factor is based on observations showing that that reduction in aerosol loading

Deleted: s

Deleted:

Deleted: is

709 between polluted days and clean days is generally tenfold over Seoul and Houston(Lance et al., 2009;
710 Kim et al., 2014). This simulation is referred to as the low-aerosol-Seoul run for the Seoul case and the
711 low-aerosol-Houston run for the Houston case. Since the control-Seoul run and the control-Houston run
712 involve higher aerosol concentrations than the low-aerosol-Seoul run and the low-aerosol-Houston run,
713 respectively, for naming purposes, the control-Seoul run and the control-Houston run are also referred
714 to as the high-aerosol-Seoul run and the high-aerosol-Houston run, respectively.

715 In addition to the simulations described above, more simulations were performed to fulfill the goals
716 of this study (Table 1). Details of those simulations are given in the following sections.

718 4.2 The GFS simulations

719
720 Note that the GFS produces the forecast data over the globe and for this study, we use the data
721 only during the MCS period and only at grid points in the domain for each case. Stated differently, the
722 spatial scale or the extent of the analysis area is identical between the CSRM simulations and the GFS
723 simulations, although the number of grid points in the area or the domain is different between the
724 CSRM simulations and the GFS simulations due to differences in resolution between those simulations.
725 We collect GFS data in the domain and then average the data over those grid points at each of the GFS
726 time steps for each of the cases. For the comparison between the GFS and CSRM simulations at
727 specific time steps over the MCS period, these averaged data are compared to the CSRM simulations
728 for each of those steps. In case the time and domain-averaged GFS data are compared to the CSRM

Deleted: during the period

730 counterparts, these averaged data are averaged again over the MCS period and compared to their
 731 CSRМ counterparts.

733 5. Results

735 5.1 Test on the effects of resolution on the simulations of clouds, 736 precipitation, and CAPI

738 5.1.1 CLC and CIC

739
 740 To test the effects of resolution on the simulations of clouds, precipitation, and their interactions with
 741 aerosols, we repeat the standard CSRМ runs at the 500-m resolution (i.e., the high-aerosol-Seoul run,
 742 the low-aerosol-Seoul run, the high-aerosol-Houston run, and the low-aerosol-Houston run) by using
 743 15- and 35-km resolutions instead. These resolutions are similar to those generally adopted by current
 744 NWP models (e.g., the GFS model). To isolate the effects of resolution on the simulations of clouds,
 745 precipitation, and their interactions with aerosols, only resolution varies among the CSRМ runs at the
 746 fine resolution and the repeated runs at the coarse resolutions here and these runs have an identical
 747 model setup except for resolution. For the identical setup, as an example, we do not apply the
 748 convection parameterizations (e.g., cumulus parameterizations) to the repeated runs, since the
 749 convection parameterizations are not applied to the CSRМ runs. Hence, cloud variables (e.g., the

Deleted: Cloud liquid content (

Deleted:)

Deleted: cloud ice content (

Deleted:)

Deleted: and thus comparisons between these repeated simulations and the CSRМ simulations can evaluate how coarse resolutions adopted by the NWP models affect the simulations of clouds, precipitation, and their interactions with aerosols

759 updraft speed) are not diagnosed by convection parameterizations but predicted in both the CSR
 760 runs and the repeated runs. With the identical setup except for resolution, the comparisons between the
 761 CSRM simulations and the repeated simulations can isolate the pure effects of the use of coarse
 762 resolution on clouds, precipitation, and their interactions with aerosol.

763 ____ The repeated simulations at the 15-km resolution are referred to as the high-aerosol-15-Seoul run,
 764 the low-aerosol-15-Seoul run, the high-aerosol-15-Houston run, and the low-aerosol-15-Houston run,
 765 while the repeated simulations at the 35-km resolution are referred to as the high-aerosol-35-Seoul run,
 766 the low-aerosol-35-Seoul run, the high-aerosol-35-Houston run, and the low-aerosol-35-Houston run. In
 767 this study, simulations whose name includes “high-aerosol” represent the polluted scenario, while those
 768 whose name includes “low-aerosol” represent the clean scenario. In the following, we describe results
 769 from the standard and repeated simulations. For the Houston case, no clouds form at the 35-km
 770 resolution, so the description of results is only done for results at the 15-km resolution.

771 Figures 3a and 3b show the vertical distributions of the time- and domain-averaged CLC in the
 772 simulations for the Seoul case and the Houston case, respectively. Figures 4a and 4b show the vertical
 773 distributions of the time- and domain-averaged CIC in the simulations for the Seoul case and the
 774 Houston case, respectively. There are increases in the cloud mass (represented by CLC and CIC) with
 775 increasing aerosol concentration between the polluted scenario and the clean scenario not only for both
 776 the Seoul and Houston cases but also at all resolutions considered. The cloud mass is substantially less
 777 at the 15- and 35-km resolutions compared to that in the simulations at the 500-m resolution. In
 778 addition, increases in the cloud mass with increasing aerosol concentration reduce substantially as

Deleted: here are substantial decreases in t

Deleted: e cloud mass

Deleted:

782 resolution coarsens. At the 500-m resolution, on average, there is about a ~30–50% increase in cloud
 783 mass, while at the 15- or 35-km resolutions, there is only a ~2–5% increase in cloud mass in both cases.

784 For both the Seoul and Houston cases, comparisons between the cloud mass produced by the
 785 GFS simulations and that produced by the ARW simulations show that the GFS-simulated cloud mass
 786 is similar to that in the ARW simulations at the 15- and 35-km resolutions. However, the GFS-
 787 simulated cloud mass is much smaller than that in the ARW simulations at the 500-m resolution, i.e.,
 788 the CSRMs simulations. This suggests that coarse resolution used in the GFS simulations is an important
 789 cause of the differences in cloud mass between the CSRMs simulations and the GFS simulations.

Deleted: the

Deleted: the

Deleted: s

Deleted: are

791 5.1.2 Liquid water path (LWP) and ice water path (IWP)

792
 793 Figures 5a and 5b show the time series of the domain-averaged LWP and IWP for the Seoul case while
 794 Figures 6a and 6b show the same for the Houston case. Note that LWP and IWP are the vertical
 795 integrals of CLC and CIC, respectively. Consequently, the same behavior as that of CLC and CIC is
 796 seen, namely, there are increases in LWP and IWP with increasing aerosol concentrations between the
 797 polluted and clean scenarios at all resolutions, while there are less LWP and IWP with the use of the 15-
 798 and 35-km resolutions compared to using the 500-m resolution. Also, the sensitivity of LWP and IWP
 799 to increasing aerosol concentrations reduces significantly as resolution coarsens.

Deleted: decreases in

Deleted: the

800 In Figures 5 and 6, satellite-observed LWP and IWP for both cases follow reasonably well their
 801 CSRMs-simulated counterparts for the polluted scenario. This shows that the CSRMs simulations, which

808 are performed with the 500-m resolution, perform well and can thus represent benchmark
 809 simulations. The GFS-produced LWP and IWP are similar to those in the ARW simulations at the 15-
 810 and 35-km resolutions and are much smaller in magnitude than those from the CSRSM simulations and
 811 observations. Hence, the discrepancy in LWP and IWP between the GFS simulations and the CSRSM
 812 simulations or that between the GFS simulations and observations is closely linked to coarse resolution
 813 adopted by the GFS simulations. Taking the CSRSM simulations as benchmark simulations, we see that
 814 the GFS simulations underestimate the cloud mass compared to observations mainly due to coarse
 815 resolution adopted by the GFS model.

Deleted: the

Deleted: the

816 Among the ARW simulations, the sensitivity of the cloud mass to increasing aerosol
 817 concentrations reduces considerably with coarsening resolution. CSRSM simulations are benchmark
 818 simulations so the sensitivity in the CSRSM simulations is the benchmark sensitivity. Note that the GFS
 819 simulation results and the ARW simulations at the coarse resolutions of 15 and 35 km are similar. Their
 820 sensitivities are thus also likely similar, i.e., the sensitivity of the cloud mass to increasing aerosol
 821 concentrations in the GFS simulation is likely to be underestimated compared to the benchmark
 822 sensitivity of the CSRSM simulations.

Deleted: r.

Deleted:

Deleted: ¶

824 5.1.3 Updrafts, condensation, and deposition

825
 826 To understand the response of the cloud mass to increasing aerosol concentrations, and the variation in
 827 the cloud mass and its response to increasing aerosol concentrations with varying resolution, as shown in

Deleted: s

834 Figures 3, 4, 5, and 6, we calculate updraft mass fluxes since these fluxes control supersaturation that
835 in turn controls condensation and deposition as key determination factors for the cloud mass. Updraft
836 mass fluxes are obtained by multiplying the predicted updraft speed by air density. Since there are
837 negligible differences in air density among the ARW simulations, most of differences in updraft mass
838 fluxes among the simulations are caused by differences in the updraft speed or updrafts. Those
839 differences in air density are in general ~ two orders of magnitude smaller than those in the updraft
840 speed or updrafts. We also obtain condensation and deposition rates. The vertical distributions of the
841 time- and domain-averaged updraft mass fluxes, condensation rates, and deposition rates for the Seoul
842 and Houston cases are shown in Figures 7, 8, and 9, respectively. Here, condensation and deposition
843 rates are defined as the rates of changes in liquid mass and ice mass in a unit volume of air and for a
844 unit time due to condensation and deposition on the surface of hydrometeors, respectively.

845 As seen for the cloud mass, updraft mass fluxes, and condensation and deposition rates increase
846 with increasing aerosol concentrations between the polluted scenario and the clean scenario at all
847 resolutions and for all cases considered. Increasing aerosol concentrations alter cloud microphysical
848 properties such as drop size and autoconversion. Aerosol-induced changes in autoconversion in turn
849 increase cloud-liquid mass as a source of evaporation and freezing. Numerous studies (e.g., Khain et al.,
850 2005; Seifert and Beheng, 2006; Tao et al., 2007, 2012; van den Heever and Cotton, 2007; Storer et al.,
851 2010; Lee et al., 2013, 2017) have shown that aerosol-induced increases in cloud-liquid mass and
852 associated increases in freezing of cloud liquid enhance the freezing-related latent heating and thus
853 parcel buoyancy, and this invigorates convection or increases updraft mass fluxes. Those studies have

854 also shown that the aerosol-induced increases in cloud-liquid mass and associated increases in the
 855 evaporation of cloud liquid enhance the evaporation-related latent cooling and thus negative buoyancy.
 856 This intensifies downdrafts and after reaching the surface, the intensified downdrafts spread out toward
 857 the surrounding warm air to form intensified gust fronts and then, to uplift the warm air more strongly.
 858 More strongly uplifted warm air leads to invigorated convection or increased updraft mass fluxes. These
 859 freezing- and evaporation-related invigoration mechanisms are operative to induce the aerosol-induced
 860 enhancement of updraft mass fluxes, condensation, and deposition in this study.

861 _____ Aerosol-induced percentage increases in updraft mass fluxes, and deposition and condensation
 862 rates at the 500-m resolution between the polluted scenario and the clean scenario are approximately
 863 one order of magnitude greater than those at the 15- and 35-km resolutions. Stated differently, the
 864 sensitivity of updraft mass fluxes to increasing aerosol concentrations reduces substantially with
 865 coarsening resolution and due to this, the sensitivity of deposition and condensation rates, and thus the
 866 cloud mass, to increasing aerosol concentrations also reduces substantially with coarsening resolution.

867 Similar to the situation with the cloud mass, the GFS-produced updraft mass fluxes are much smaller
 868 than those produced by the ARW simulations at the 500-m resolution (or the CSRMs simulations) and
 869 similar to those produced by the ARW simulations at the 15- and 35-km resolutions (Figure 7). Hence,

870 taking the CSRMs simulations as benchmark simulations, the updraft mass fluxes (and thus the cloud
 871 mass) are underestimated in the GFS simulations and the ARW simulations at the 15- and 35-km
 872 resolutions. This underestimation is closely linked to the discrepancy in resolution between the GFS
 873 simulations and the CSRMs simulations or between the ARW simulations at the 15- and 35-km

Deleted: km

Deleted:

Deleted: the discrepancy in updraft mass fluxes between the GFS simulations and the CSRMs simulations

Deleted: s

Deleted: s

881 resolutions and the CSR simulation. Taking the sensitivity of updraft mass fluxes to increasing
 882 aerosol concentrations in the CSR simulation as the benchmark sensitivity, the GFS simulations
 883 likely also underestimate the sensitivity. considering the similarity in results between the ARW
 884 simulations at the 15- and 35-km resolutions and the GFS simulations. Since the current GFS model
 885 does not consider pathways through which increasing aerosol concentrations interact with updraft mass
 886 fluxes, this probable underestimation of the sensitivity is even more likely. Note that the ARW
 887 simulations which are at the 15- and 35-km resolutions and underestimate updrafts themselves, even
 888 with the consideration of those pathways, result in the much weaker sensitivity at the coarse resolutions
 889 as compared to that in the CSR simulation. Hence, even though those pathways are implemented
 890 into the GFS model, the underestimated updrafts in the GFS simulations are likely to result in the weak
 891 sensitivity, unless the cumulus parameterization which represents updrafts in the GFS model is further
 892 developed to prevent the underestimation of updrafts.

Deleted: e two types of simulations. The underestimation of the updraft mass fluxes in the GFS simulations is mainly due to the coarse resolution adopted by the GFS model.

Deleted: .

893 Figure 10 shows the frequency distribution of updrafts over the updraft speed, which is normalized
 894 over the domain and the simulation period. We first calculate the frequency over the domain at each
 895 time step and in each discretized updraft bin. The frequency in each bin and at each time step is then
 896 divided by the total number of grid points in the whole domain. The normalized frequency at each time
 897 step is summed over all of the time steps in each updraft bin. This sum is divided by the total number of
 898 time steps as the final step in the normalization process. With coarsening resolution, the normalized
 899 frequency of weak updrafts with speeds less than $\sim 2 \text{ m s}^{-1}$ increases for both scenarios in both cases.
 900 However, the normalized frequency of strong updrafts with speeds greater than $\sim 2 \text{ m s}^{-1}$ reduces with

Deleted: ¶

907 coarsening resolution. The frequency shift from high-level updraft speeds to low-level speeds leads
 908 to a reduction in the mean updrafts with coarsening resolution for both scenarios in both cases.

909 The updraft frequency is greater in the polluted scenario than in the clean scenario at all
 910 resolutions and for all cases. The overall difference in the frequency between the scenarios reduces with
 911 coarsening resolution. This is associated with the reduction in the sensitivity of the averaged updrafts to
 912 increasing aerosol concentrations with coarsening resolution. In particular, the difference in the
 913 frequency for weak updrafts (speeds less than $\sim 2 \text{ m s}^{-1}$) between the scenarios does not vary much with
 914 coarsening resolution. On average, the percentage difference for weak updrafts is less than 2–3% at all
 915 resolutions. However, the difference for strong updrafts varies significantly with varying resolution.
 916 The mean difference for strong updrafts varies from $\sim 30\text{--}60\%$ for the 500-m resolution to less than $\sim 5\text{--}$
 917 6% for the 15- and 35-km resolutions. Analyses of the updraft frequency here suggest that strong
 918 updrafts are more sensitive to aerosol-induced invigoration of convection than weak updrafts. The
 919 variation in the sensitivity of the averaged updrafts to increasing aerosol concentrations at varying
 920 resolution is associated more with the variation of the response of strong updrafts to aerosol-induced
 921 invigoration at varying resolution than with that of weak updrafts. Another point to make here is that
 922 the frequency of weak updrafts is overestimated while that of strong updrafts is underestimated at
 923 coarse resolution compared to the frequencies in the fine-resolution CSRM simulations.

Deleted: Numerous studies (e.g., Khain et al., 2005; Seifert and Beheng, 2006; Tao et al., 2007, 2012; van den Heever and Cotton, 2007; Storer et al., 2010; Lee et al., 2013, 2017) have shown that aerosol-induced invigoration of convection through aerosol-induced increases in freezing or aerosol-induced intensification of gust fronts is the main mechanism behind aerosol-induced increases in updraft mass fluxes or the intensity of updrafts. Based on this,

Deleted: a

Deleted: s

Deleted: s

Deleted: s

5.1.4 Evaporation and precipitation distributions

941 Aerosol-induced increases in evaporation and associated cooling affect downdrafts, and changes in
942 downdrafts in turn affect gust fronts. Aerosol-induced changes in the intensity of gust fronts affect the
943 organization of cloud systems, which is characterized by cloud-cell spatiotemporal distributions. In
944 general, aerosol-induced greater increases in evaporation result in aerosol-induced greater changes in
945 the intensity of gust fronts and in cloud system organization (Tao et al., 2007, 2012; van den Heever
946 and Cotton, 2007; Storer et al., 2010; Lee et al., 2013, 2017).

947 Considering that individual cloud cells act as individual sources of precipitation, aerosol-induced
948 changes in the cloud system organization can alter precipitation spatiotemporal distributions, which
949 play an important role in hydrological circulations. It is thus important to examine how the response of
950 evaporation to increasing aerosol concentrations varies with varying resolution, i.e., to see how coarse
951 resolution affects the quality of simulations of aerosol effects on hydrological circulations. Motivated
952 by this, evaporation rates are obtained and are shown in Figure 11. Here, evaporation rate is defined as
953 the rate of changes in liquid mass in a unit volume of air and for a unit time due to evaporation on the
954 surface of hydrometeors.

Deleted: s

955 As seen in the above-described variables, evaporation rates increase as the aerosol concentration
956 increases and the sensitivity of the evaporation rate to increasing aerosol concentrations reduces with
957 coarsening resolution among the ARW simulations. This suggests that the sensitivities of the cloud
958 system organization and precipitation distributions to increasing aerosol concentrations likely also
959 reduce with coarsening resolution, as reported in the previous studies (e.g., Tao et al., 2007, 2012; van
960 den Heever and Cotton, 2007; Storer et al., 2010; Lee et al., 2013, 2017). This is confirmed by the

962 distribution of normalized precipitation frequency over precipitation rates shown in Figure 12.

963 Similar to the normalization for the updraft frequency, we first calculate the frequency of surface

964 precipitation rates at each time step and in each discretized precipitation rate bin. The frequency in each

965 bin and at each time step is then divided by the total number of grid points at the surface. The

966 normalized frequency at each time step is summed over all of the time steps. This sum is divided by the

967 total number of time steps as the final step in the normalization process. Figure 12 shows that due to the

968 reduction in the sensitivity of evaporative cooling to increasing the aerosol concentration as resolution

Deleted: the

969 coarsens, differences in the distribution of precipitation frequency between the polluted scenario and the

970 clean scenario reduce substantially as resolution coarsens. Taking the 500-m resolution CSR

Deleted: the

971 simulations as benchmark simulations, this suggests that the coarse-resolution GFS simulations likely

972 underestimate the sensitivity of evaporative cooling, cloud system organization, and precipitation

973 distributions to increasing aerosol concentrations.

974

975 **5.2 Test on the effects of microphysics parameterizations on the simulations of clouds,**

976 **precipitation, and CAPI**

977

978 As mentioned previously, among microphysical processes, saturation, sedimentation, and collection

979 processes are those whose parameterizations are a main cause of errors in the simulation of clouds,

980 precipitation, and CAPI. Motivated by this, we focus on these three microphysical processes for testing

981 the effects of microphysics parameterizations on the simulations of clouds, precipitation, and CAPI. As

984 a preliminary step to this test, we first focus on the effects of microphysics parameterizations on the
985 simulation of the cloud mass, which plays a key role in cloud radiative properties and precipitation.
986 Based on Figures 3 and 4, we focus on the CLC, which accounts for the bulk of the total cloud mass.

987 Figure 13 shows the vertical distributions of the time- and domain-averaged CLC. In Figure 13a,
988 solid red and black lines represent the high-aerosol-Seoul run and the low-aerosol-Seoul run,
989 respectively, while in Figure 13b, those lines represent the high-aerosol-Houston run and the low-
990 aerosol-Houston run, respectively. Note that these runs shown in the figure are performed using the bin
991 scheme and the 500-m resolution. These simulations were repeated with the Morrison two-moment
992 scheme. These repeated simulations using the MG scheme, referred to as the high-aerosol-MG-Seoul
993 run, the low-aerosol-MG-Seoul run, the high-aerosol-MG-Houston run and the low-aerosol-MG-
994 Houston run, are represented by solid yellow and green lines in Figure 13. Between the high-aerosol
995 and low-aerosol runs using the MG scheme for the two cases, there is an increase in CLC with
996 increasing aerosol concentration. However, this increase is much smaller than that between the high-
997 aerosol and low-aerosol runs using the bin scheme for the two cases. In addition, there is a significant
998 difference in the shape of the vertical profile of CLC between the simulations with the MG scheme and
999 those with the bin scheme for both cases. Here, the shape is represented by the peak value of CLC and
1000 the altitude of the peak value in the vertical profile. The peak value is higher in the simulations with the
1001 bin scheme than in the simulations with the MG scheme for each of the polluted and clean scenarios.
1002 The altitude of the peak value is lower in the simulations with the bin scheme than in the simulations

1003 with the MG scheme. For the Seoul (Houston) case, the altitude is ~ 2 (3) km in the simulations with
1004 the bin scheme, while it is ~ 5 km in those with the MG scheme.

1005 We next test how the parameterization of saturation processes affects the simulations by
1006 comparing the supersaturation prediction in the bin scheme to the saturation adjustment in the MG
1007 scheme. To do this, the simulations with the bin scheme are repeated after replacing the supersaturation
1008 prediction in the bin scheme with the saturation adjustment in the MG scheme. These repeated
1009 simulations are referred to as the high-aerosol-sat-Seoul run, the low-aerosol-sat-Seoul run, the high-
1010 aerosol-sat-Houston run, and the low-aerosol-sat-Houston run. The high-aerosol-sat-Seoul run and the
1011 low-aerosol-sat-Seoul run for the Seoul case and the high-aerosol-sat-Houston run and the low-aerosol-
1012 sat-Houston run for the Houston case are represented by dashed lines in Figure 13. As in the other
1013 simulations, there is an increase in CLC with increasing aerosol concentrations between the high-
1014 aerosol-sat and the low-aerosol-sat runs for the two cases. However, this increase is much smaller than
1015 that between the high-aerosol and low-aerosol runs for the two cases, but is similar to that between the
1016 high-aerosol-MG and low-aerosol-MG runs for the two cases. This suggests that the sensitivity of the
1017 CLC to increasing aerosol concentrations is affected by the parameterization of the saturation process
1018 and that the use of the saturation adjustment reduces the sensitivity compared to using the
1019 supersaturation prediction.

1020 The high-aerosol-sat-Seoul run, the low-aerosol-sat-Seoul run, the high-aerosol-sat-Houston run,
1021 and the low-aerosol-sat-Houston run are repeated by replacing the bin-scheme sedimentation with the
1022 sedimentation from the MG scheme as a way of testing the effects of the parameterization of

1023 sedimentation on the simulations. These repeated runs are referred to as the high-aerosol-sed-Seoul
1024 run, the low-aerosol-sed-Seoul run, the high-aerosol-sed-Houston run, and the low-aerosol-sed-Houston
1025 run. These runs are identical to the high-aerosol-Seoul run, the low-aerosol-Seoul run, the high-aerosol-
1026 Houston run and the low-aerosol-Houston run, respectively, except for the parameterization of the
1027 saturation and sedimentation processes. As mentioned previously, terminal velocities vary as
1028 hydrometeor sizes vary in the bin scheme, while the MG scheme adopts mass-weight mean terminal
1029 velocities for the calculation of the sedimentation process.

1030 The vertical distributions of the CLC in the high-aerosol-sed-Seoul run, the low-aerosol-sed-Seoul
1031 run, the high-aerosol-sed-Houston run, and the low-aerosol-sed-Houston run are represented by dashed
1032 lines in Figure 14. Comparisons between the pair of high-aerosol-sed and low-aerosol-sed runs for the
1033 two cases and the pair of high-aerosol-MG and low-aerosol-MG runs for the two cases show that not
1034 only the increases in the CLC with increasing aerosol concentrations but also the shapes of the vertical
1035 distribution of the CLC in the high-aerosol-sed and low-aerosol-sed runs for the two cases are similar to
1036 those in the high-aerosol-MG and low-aerosol-MG runs for the two cases. This demonstrates that
1037 differences in the shape of the vertical profile of CLC between the bin-scheme simulations and the MG-
1038 scheme simulations are not explained by differences in the representation of the saturation process
1039 alone. This also demonstrates that the representation of the sedimentation process plays an important
1040 role in generating the differences in the shape of the vertical profile of CLC.

1041 In Figure 14, we still see differences in the vertical profiles of CLC between the high-aerosol-sed-
1042 Seoul and high-aerosol-MG-Seoul runs, and between the low-aerosol-sed-Seoul and low-aerosol-MG-

1043 Seoul runs, as well as between the high-aerosol-sed-Houston and high-aerosol-MG-Houston runs,
1044 and between the low-aerosol-sed-Houston and low-aerosol-MG-Houston runs. To understand the cause
1045 of these differences, the high-aerosol-sed-Seoul run, the low-aerosol-sed-Seoul run, the high-aerosol-
1046 sed-Houston run, and the low-aerosol-sed-Houston run are repeated again with the MG-scheme
1047 collection process. These repeated runs are referred to as the high-aerosol-col-Seoul run, the low-
1048 aerosol-col-Seoul run, the high-aerosol-col-Houston run, and the low-aerosol-col-Houston run. These
1049 runs are identical to the high-aerosol-Seoul run, the low-aerosol run-Seoul, the high-aerosol-Houston
1050 run, and the low-aerosol-Houston run, respectively, except for the parameterization of the saturation,
1051 sedimentation, and collection processes. As mentioned previously, collection efficiencies vary as
1052 hydrometeor sizes vary in the bin scheme, while the MG scheme uses constant collection efficiencies.

1053 As seen in Figure 15, the remaining differences between the high-aerosol-col-Seoul and high-
1054 aerosol-MG-Seoul runs and between the low-aerosol-col-Seoul and low-aerosol-MG-Seoul runs, as
1055 well as between the high-aerosol-col-Houston and high-aerosol-MG-Houston runs, and between the
1056 low-aerosol-col-Houston and low-aerosol-MG-Houston runs nearly disappear. This demonstrates with
1057 fairly good confidence that differences between the high-aerosol-Seoul run (the high-aerosol-Houston
1058 run) and the high-aerosol-MG-Seoul run (the high-aerosol-MG-Houston run) or between the low-
1059 aerosol-Seoul run (the low-aerosol-Houston run) and the low-aerosol-MG-Seoul run (the low-aerosol-
1060 MG-Houston run) are explained by differences in the parameterizations of the saturation,
1061 sedimentation, and collection processes between the bin scheme and the MG scheme.

5.3 Relative importance of resolution and parameterizations

Comparisons between ARW simulations with different resolutions and those with different microphysics parameterizations as shown in Figures 3 and 13 demonstrate that the variation in cloud variables is much greater with respect to the variation in resolution than with the variation in microphysics parameterizations. For example, comparisons between Figures 3 and 13 show that the variation in the time- and domain-averaged cloud mass is $\sim 2\text{--}4$ times greater as resolution varies than when the microphysics parameterizations varies. These comparisons also show that the variation in cloud variables with varying resolution explains the discrepancy between the GFS simulations and the CSRM simulations and between the GFS simulations and observations much better than the variation in microphysics parameterizations. As a first step toward reducing the first-order errors in the GFS simulations, we first need to focus on the reduction in errors that are associated with the use of coarse resolution in the GFS model.

Deleted: the

Deleted: s

Deleted: s

6. Summary and Discussion

This study examines the uncertainties in the simulations of clouds, precipitation, and CAPI in the NWP models. Here, we focus on those uncertainties that are created by the microphysics parameterizations and by the model resolution chosen. In particular, for the examination of the uncertainties associated

1085 with microphysics parameterizations, we investigate the contributions of the parameterizations of
1086 three key microphysical processes, i.e., saturation, collection, and sedimentation, to the uncertainties.

1087 As a way of examining the uncertainties created by the microphysics parameterizations, we
1088 compare the MG scheme (a representative bulk scheme) to the bin scheme, which acts as a benchmark
1089 scheme. The vertical distribution of the cloud mass simulated by the MG scheme deviates substantially
1090 from that simulated by the bin scheme. In particular, there is a substantial discrepancy in the peak value
1091 of the distribution and the altitude of the peak value between the schemes. Also, there is a substantial
1092 discrepancy between the schemes in the sensitivity of the cloud mass to increasing aerosol
1093 concentrations.

1094 The discrepancy in the sensitivity is closely linked to the discrepancy in the parameterization of the
1095 saturation processes between the schemes. The use of the saturation adjustment in the bulk scheme
1096 reduces the sensitivity by a factor of ~ 2 compared to the use of the supersaturation prediction in the bin
1097 scheme. The discrepancy in the peak value and its altitude between the schemes is strongly linked to the
1098 parameterization of sedimentation in the schemes. The use of identical parameterizations of saturation
1099 and sedimentation makes the sensitivity and the peak value and its altitude similar between the schemes,
1100 although there still remains a slight difference in the magnitude of the cloud mass. This remaining
1101 difference is explained by the discrepancy in the parameterization of the collection process. When the
1102 two schemes use identical parameterizations of the saturation, sedimentation, and collection processes,
1103 the sensitivity and the peak value and its altitude become nearly identical between the two schemes.
1104 This confirms that differences in the parameterizations of the three key processes (i.e., saturation,

1105 sedimentation, and collection) are the main cause of the differences in the simulations of clouds
 1106 between the schemes as indicated by Fan et al. (2012) and Khain et al. (2015).

1107 By selecting the simulations with the bin scheme as benchmark simulations, we see that the use
 1108 of the saturation adjustment, as done in most current NWP models, can lead to an underestimation of
 1109 the sensitivity of the cloud mass to increasing aerosol concentrations. Fan et al. (2012) and Khain et al.
 1110 (2015) have also shown that the sensitivity of the cloud mass to increasing aerosol concentrations is
 1111 lower in the bulk scheme than in the bin scheme. This study shows that the lower sensitivity in the bulk
 1112 scheme is closely linked to the use of the saturation adjustment in the bulk scheme.

1113 It is well known that the shape of the vertical profile of the cloud mass (i.e., the peak value of the
 1114 cloud mass and its altitude) or how cloud mass is distributed in the vertical domain has substantial
 1115 implications for cloud radiative forcing and precipitation processes. This study demonstrates that the
 1116 different parameterizations of the sedimentation process between the schemes lead to different shapes
 1117 of the cloud-mass profiles and thus different cloud radiative forcings and precipitation processes. The
 1118 use of a mass-weight mean terminal velocity for sedimentation as done in the bulk schemes can lead to
 1119 misleading shapes, cloud radiative forcings, and precipitation processes compared to those in the
 1120 benchmark bin-scheme simulations where terminal velocities vary as hydrometeor sizes vary.

1121 NWP models (e.g., the GFS model) adopt coarse resolution. This study shows that the use of
 1122 coarse resolution can cause an underestimation of the updraft intensity and thus condensation and
 1123 deposition, which leads to an underestimation of the cloud mass. Also, the use of coarse resolution
 1124 likely results in the underestimation of the sensitivity of updrafts and cloud mass and that of

Deleted: s

Deleted: s

Deleted: supersaturation

Deleted: ,

Deleted: s

1130 evaporation, cloud system organization, and precipitation distributions to increasing aerosol
 1131 concentrations.

1132 Through the examination of the sensitivity of the results to ~~resolution~~ chosen, we find that
 1133 updrafts, associated other cloud variables, and their sensitivity to increasing aerosol concentrations are
 1134 strongly controlled by small-scale updrafts. When they are resolved with the use of high-resolution
 1135 models, there are high-~~value~~, averaged updrafts ~~and~~, associated variables, and their ~~strong~~ sensitivity but
 1136 when they are not resolved in low-resolution models, there are low-~~value~~, averaged updrafts ~~and~~,
 1137 associated variables, and their ~~weak~~ sensitivity. This means that small-scale updrafts not resolved with
 1138 coarse resolution, ~~play an important role in the simulation of the correct magnitude of updrafts,~~
 1139 associated variables, and their sensitivity to increasing aerosol concentrations.

1140 The frequency distributions of updrafts simulated in this study show that the frequency of weak
 1141 updrafts is overestimated while that of strong updrafts is underestimated in the simulations with coarse
 1142 resolution, ~~compared to those in the CSRM simulations. Hence, the updraft speed shifts toward lower~~
 1143 values with coarsening resolution. The difference in the frequency between the polluted and clean
 1144 scenarios reduces substantially, particularly for strong updrafts, with coarsening resolution. This is why
 1145 the sensitivity of updrafts and associated cloud variables to increasing aerosol concentrations reduces
 1146 with coarsening resolution. We see that not resolving small-scale updrafts results in the underestimation
 1147 of strong updrafts and the overestimation of weak updrafts for both scenarios and in the reduced
 1148 difference in strong updrafts between the scenarios.

Deleted: the

Deleted: level

Deleted: ,

Deleted: level

Deleted: ,

Deleted: s

Deleted: s

1156 The GFS simulations use the so-called sub-grid parameterizations (e.g., cumulus
1157 parameterizations) that represent sub-grid updrafts and associated variables, while the ARW
1158 simulations at the 500-m resolution (i.e., the CSRМ simulations) do not use these sub-grid
1159 parameterizations based on consideration that the CSRМ simulations resolve sub-grid processes. Thus,
1160 the CSRМ simulations (that prove to act as benchmark simulations through comparisons to
1161 observations) are able to evaluate the sub-grid parameterizations in the GFS model. The sub-grid
1162 parameterizations are designed to correct errors that are caused by the use of coarse resolution in the
1163 GFS model. However, comparisons between the GFS simulations and the ARW simulations at different
1164 resolutions indicate that despite the presence of sub-grid parameterizations in the GFS model, the errors
1165 or differences in the updraft intensity and associated cloud variables between the GFS simulations and
1166 the CSRМ simulations exist due to resolution. Hence, sub-grid parameterizations need to be improved
1167 to better represent sub-grid processes. To this end, results here indicate that sub-grid parameterizations
1168 (e.g., scale-aware cumulus schemes) which are being implemented into the NWP models (e.g., the GFS
1169 model) should be able to compensate for the over- and under-estimation of weak updrafts and strong
1170 updrafts, respectively, due to coarse resolution.

Deleted: s

Deleted: s

Deleted: s

1171 Comparisons between the GFS simulations and the ARW simulations also indicate that it is
1172 likely that the GFS model underestimates the sensitivity of updrafts and associated cloud variables to
1173 increasing aerosol concentrations. In general, parameterizations that represent sub-grid updrafts and
1174 other associated variables do not have pathways through which increasing aerosol concentrations affect
1175 updrafts and associated cloud variables. However, recent studies by Lim et al. (2014), Thayer-Calder et

1179 al. (2015), and Griffin and Larson (2016) have attempted to consider interactions among
1180 microphysical processes, their variations with varying aerosol concentrations, and sub-grid dynamic
1181 (e.g., updrafts and downdrafts) and thermodynamic (e.g., temperature) variables in those
1182 parameterizations. These efforts should focus on countering the variation in the sensitivity of updrafts,
1183 in particular strong updrafts and thus that of cloud variables, cloud system organization, and
1184 precipitation distributions to increasing aerosol concentrations with coarsening resolution. While the
1185 pattern of the sensitivity and its variation shown in this study provides valuable information useful for
1186 aiding these efforts, results may be different for different cloud types and environments, given the
1187 strong dependence of aerosol-cloud interactions on cloud type and environmental conditions. So to aid
1188 the efforts in a generalized way, future studies with more cases that involve various types of aerosol-
1189 cloud interactions are needed.

1190

1191

1192

1193

1194

1195

1196

1197

1198

1199

1200

Acknowledgements. This study is supported by NOAA (Grant NOAA-NWS-NWSP0-2015-2004117), which also provided the GFS forecast data, and Korea Environmental Industry & Technology Institute funded by the Korea Ministry of Environment as “Climate Change Correspondence Program”. This study is also supported by “Development of Climate and Atmospheric Environmental Applications” project, funded by ETRI, which is a subproject of “Development of Geostationary Meteorological Satellite Ground Segment (NMSC-2017-01)” program funded by NMSC of KMA.

Deleted: .

1201
1202
1203
1204
1205
1206
1207
1208
1209
1210
1211
1212
1213
1214
1215
1216
1217
1218
1219
1220
1221
1222
1223
1224

References

- Basu S, Z. N. Begum, E. N. Rajagopal, 1998, [Impact of boundary-layer parameterization schemes on the prediction of the Asian summer monsoon. *Boundary-Layer Meteorol.* 86, 469–485.](#)
- Bogenschutz, P. A., and S. K. Krueger, 2013, A simplified PDF parameterization of subgrid-scale clouds and turbulence for cloud-resolving models, *J. Adv. Model. Earth Syst.*, 5, 195–211, doi:10.1002/jame.20018.
- Donelan, M. A., B. K. Haus, N. Reul, et al., 2004, On the limiting aerodynamic roughness of the ocean in very strong winds. *Geophys. Res. Lett.*, 31, doi: 10.1029/2004GL019460.
- Griffin, B. M. and V. E. Larson, 2016, Parameterizing microphysical effects on variances and covariances of moisture and heat content using a multivariate probability density function: a study with CLUBB (tag MVCS), *Geosci. Model Dev.*, 9, 4273–4295, doi:10.5194/gmd-9-4273-2016.
- Hwang, S.-O., and D.-K. Lee, 1993, A study on the relationship between heavy rainfalls and associated low-level jets in the Korean peninsula, *J. Korean Meteorol. Soc.*, 29, 133–146.
- Fan J, T. Yuan, J. M. Comstock, et al., 2009. Dominant role by vertical wind shear in regulating aerosol effects on deep convective clouds." *J. Geophys. Res.*, 114, doi:10.1029/2009JD012352.
- Fan, J., L. R. Leung, Z. Li, H. Morrison, et al., 2012, Aerosol impacts on clouds and precipitation in eastern China: Results from bin and bulk microphysics, *J. Geophys. Res.*, 117, D00K36, doi:10.1029/2011JD016537.
- Fan, J., L.R. Leung, D. Rosenfeld, Q. Chen, Z. Li, J. Zhang, H. Yan, 2013, Microphysical effect determine macrophysical response for aerosol impact on deep convective clouds, *Proceedings of National Academy of Sciences (PNAS)*, doi:10.1073/pnas.1316830110.
- Fouquart, Y., and B. Bonnel, B., 1980, Computations of solar heating of the Earth's atmosphere: A new parameterization, *Beitr. Phys. Atmos.*, 53, 35-62.
- Khain, A. P., D. Rosenfeld, and A. Pokrovsky, 2005, Aerosol impact on the dynamics and microphysics of deep convective clouds, *Q. J. R. Meteorol. Soc.*, 131, 2639–2663, doi:10.1256/qj.04.62.
- Khain, A., and B. Lynn, 2009, Simulation of a supercell storm in clean and dirty atmosphere using weather research and forecast model with spectral bin microphysics, *J. Geophys. Res.*, 114, D19209, doi:10.1029/2009JD011827.
- Khain, A. P., et al., 2015, Representation of microphysical processes in cloud-resolving models: Spectral (bin) microphysics versus bulk parameterization, *Rev. Geophys.*, 53, 247–322, doi:10.1002/2014RG000468.
- Kim, J. H., S. S. Yum, S. Shim, et al., 2014, On the submicron aerosol distributions and CCN number concentrations in and around the Korean Peninsula, *Atmos. Chem. Phys.*, 14, 8763–8779, doi:10.5194/acp-14-8763-2014.
- Lance, S., A. Nenes, C. Mazzoleni, et. al., 2009, Cloud condensation nuclei activity, closure, and droplet growth kinetics of Houston aerosol during the Gulf of Mexico Atmospheric Composition and Climate Study (GoMACCS), *J. Geophys. Res.*, 114, D00F15,

Deleted: ¶

¶
¶
¶
¶
¶

- 1272 doi:10.1029/2008JD011699.
- 1273 Lee, S. S. and G. Feingold, 2013, Aerosol effects on the cloud-field properties of tropical convective
1274 clouds, *Atmos. Chem. Phys.*, 13, 6713-6726.
- 1275 Lee, S. S., W.-K. Tao, and C. H. Jung, 2014, Aerosol effects on instability, circulations, clouds and
1276 precipitation, *Advances in Meteorology*, Article ID 683950.
- 1277 Lee, S. S., Z. Li, J. Mok, et al., 2017, Interactions between aerosol absorption, thermodynamics,
1278 dynamics, and microphysics and their impacts on a multiple-cloud system, *Clim. Dynam.*, doi:
1279 10.1007/s00382-017-3552-x.
- 1280 Li, Z., F. Niu, J. Fan, Y. Liu, D. Rosenfeld, and Y. Ding, 2011, Long-term impacts of aerosols on the
1281 vertical development of clouds and precipitation, *Nature Geo.*, doi: 10.1038/NGEO1313.
- 1282 Lim, K. S., J. Fan, L. Y. R. Leung, et al., 2014, Investigation of aerosol indirect effects using a cumulus
1283 microphysics parameterization in a regional climate model, *J. Geophys. Res.*, 119, 906-926.
- 1284 Mlawer, E. J., S. J. Taubman, P. D. Brown, M. J. Iacono, and S. A. Clough, 1997, RRTM, a validated
1285 correlated-k model for the longwave, *J. Geophys. Res.*, 102, 16663-16682.
- 1286 Moorthi, S., H.-L. Pan, and P. Caplan, Changes to the 2001 NCEP operational MRF/AVN global
1287 analysis/forecast system, 2001, *Technical Procedures Bulletin*, 484, 14pp., obtainable at
1288 <http://www.nws.noaa.gov/om/tpb/484.htm>
- 1289 Morcrette, J.-J., A. Benedetti, A. Ghelli, J.W. Kaiser, A.M. Tompkins, 2011, Aerosol-cloud-radiation
1290 interactions and their impact on ECMWF/MACC forecasts, *Technical Memorandum*, 660, 35pp.
- 1291 Morrison, H., and A. Gettelman, 2008: A new two-moment bulk stratiform cloud microphysics scheme
1292 in the Community Atmosphere Model, version 3 (CAM3). Part I: Description and numerical
1293 tests, *J. Climate*, 21, 3642--3659, doi:10.1175/2008JCLI2105.1.
- 1294 Morrison, H., G. Thompson, and V. Tatarskii, 2009, Impact of cloud microphysics on the development
1295 of trailing stratiform precipitation in a simulated squall line: Comparison of one- and two-
1296 moment schemes, *Mon. Wea. Rev.*, 137, 991–1007.
- 1297 Pan, H.-L., and W.-S. Wu, 1995, Implementing a mass flux convective parameterization package for
1298 the NMC Medium-Range Forecast model, *NMC Office Note* 409, 40 pp.
- 1299 Randall, D. A., M. E. Schlesinger, V. Galin, V. Meleshko, J.-J. Morcrette, and R. Wetherald, 2006,
1300 Cloud Feedbacks. In "Frontiers in the Science of Climate Modeling," J. T. Kiehl and V.
1301 Ramanathan, Eds., Cambridge University Press, 217-250.
- 1302 Seifert, A., and D. Beheng, 2006, A two-moment cloud microphysics parameterization for mixed-phase
1303 clouds. Part 2: Maritime vs. continental deep convective storms, *Meteorol. Atmos. Phys.*, 92,
1304 67-82.
- 1305 Seifert, A., C. Köhler, and K. D. Beheng, Aerosol-cloud-precipitation effects over Germany as
1306 simulated by a convective-scale numerical weather prediction model, *Atmos. Chem. Phys.*, 12,
1307 709-725, doi:10.5194/acp-12-709-2012, 2012.
- 1308 Storer, R.L., S.C. van den Heever, and G.L. Stephens, 2010, Modeling aerosol impacts on convective
1309 storms in different environments, *J. Atmos. Sci.*, 67, 3904-3915.
- 1310 Sudhakar, D., J. Quaas, R. Wolke, J. Stoll, A. Mühlbauer, M. Salzmann, B. Heinold, and I. Tegen,
1311 2016, Implementation of aerosol-cloud interactions in the regional atmosphere-aerosol model

- 1312 COSMO-MUSCAT and evaluation using satellite data, *Geosci. Model Dev. Discuss.*,
1313 doi:10.5194/gmd-2016-186.
- 1314 Sun, J., T.-Y. Lee, 2002, A numerical study of an intense quasistationary convection band over the
1315 Korean peninsula, *J. Meteorol. Soc. Jpn.*, 80, 1221–1245.
- 1316 Sundqvist, H., E. Berge, and J. E. Kristjansson, 1989, Condensation and cloud parameterization studies
1317 with a mesoscale numerical weather prediction model, *Mon. Weather Rev.*, 117, 1641-1657.
- 1318 Tao, W.-K., X. Li, A. Khain, T. Matsui, S. Lang, and J. Simpson, 2007, The role of atmospheric aerosol
1319 concentration on deep convective precipitation: cloud-resolving model simulations, *J. Geophys.*
1320 *Res.*, 112, D24S18, doi:10.1029/2007JD008728.
- 1321 Tao, W.-K., J. P. Chen, Z. Li, and C. Zhang, 2012, Impact of aerosols on convective clouds and
1322 precipitation, *Rev. of Geophy.*, 50, RG2001, doi:10.1029/2011RG000369.
- 1323 Thayer-Calder, K., A. Gettelman, C. Craig, et al., 2015, A unified parameterization of clouds and
1324 turbulence using CLUBB and subcolumns in the Community Atmosphere Model, *Geosci.*
1325 *Model Dev.*, 8, 3801-3821, doi:10.5194/gmd-8-3801-2015.
- 1326 van den Heever, S.C., and W.R. Cotton, 2007, Urban aerosol impacts on downwind convective storms,
1327 *J. Appl. Meteor. Climatol.*, 46, 828-850.
- 1328 van den Heever, S. C., G. L. Stephens, and N. B. Wood, 2011, Aerosol indirect effects on tropical
1329 convection characteristics under conditions of radiative-convective equilibrium, *J. Atmos. Sci.*,
1330 68, 699-718.
- 1331 Wang, H., W. C. Skamarock, and G. Feingold, 2009, Evaluation of scalar advection schemes in the
1332 Advanced Research WRF model using large-eddy simulations of aerosol-cloud interactions,
1333 *Mon. Wea. Rev.*, 137, 2547-2558.
- 1334 Zeng, X., and A. Beljaars, 2005, A prognostic scheme of sea surface skin temperature for modeling and
1335 data assimilation, *Geophys. Res. Lett.*, 32, L14605, doi:10.1029/2005GL023030, 2005.
- 1336 Zhao, Q. Y., and F. H. Carr, 1997, A prognostic cloud scheme for operational NWP models, *Mon. Wea.*
1337 *Rev.*, 125, 1931- 1953.

1338

1339

1340

1341

1342

1343

1344

Tables

Deleted: ¶

1345

1346

1347 Table 1. Description of the simulations.

Simulations	Case	Aerosol number concentration at the surface (cm^{-3})	Microphysics scheme	Resolution	Saturation	Sedimentation	Collection
High-aerosol-Seoul run	Seoul	5500	Bin	500 m	Supersaturation prediction	Bin-scheme sedimentation	Bin-scheme collection
Low-aerosol-Seoul run	Seoul	550	Bin	500 m	Supersaturation prediction	Bin-scheme sedimentation	Bin-scheme collection
High-aerosol-Houston run	Houston	1500	Bin	500 m	Supersaturation prediction	Bin-scheme sedimentation	Bin-scheme collection
Low-aerosol-Houston run	Houston	150	Bin	500 m	Supersaturation prediction	Bin-scheme sedimentation	Bin-scheme collection
High-aerosol-15-Seoul run	Seoul	5500	Bin	15 km	Supersaturation prediction	Bin-scheme sedimentation	Bin-scheme collection
Low-aerosol-15-Seoul run	Seoul	550	Bin	15 km	Supersaturation prediction	Bin-scheme sedimentation	Bin-scheme collection
High-aerosol-15-Houston run	Houston	1500	Bin	15 km	Supersaturation prediction	Bin-scheme sedimentation	Bin-scheme collection
Low-aerosol-15-Houston	Houston	150	Bin	15 km	Supersaturation prediction	Bin-scheme sedimentation	Bin-scheme collection

run							
High-aerosol-35-Seoul run	Seoul	5500	Bin	35 km	Supersaturation prediction	Bin-scheme sedimentation	Bin-scheme collection
Low-aerosol-35-Seoul run	Seoul	550	Bin	35 km	Supersaturation prediction	Bin-scheme sedimentation	Bin-scheme collection
High-aerosol-35-Houston run	Houston	1500	Bin	35 km	Supersaturation prediction	Bin-scheme sedimentation	Bin-scheme collection
Low-aerosol-35-Houston run	Houston	150	Bin	35 km	Supersaturation prediction	MG-scheme sedimentation	MG-scheme collection
High-aerosol-MG-Seoul run	Seoul	5500	MG	500 m	Saturation adjustment	MG-scheme sedimentation	MG-scheme collection
Low-aerosol-MG-Seoul run	Seoul	550	MG	500 m	Saturation adjustment	MG-scheme sedimentation	MG-scheme collection
High-aerosol-MG-Houston run	Houston	1500	MG	500 m	Saturation adjustment	MG-scheme sedimentation	MG-scheme collection
Low-aerosol-MG-Houston run	Houston	150	MG	500 m	Saturation adjustment	MG-scheme sedimentation	MG-scheme collection
High-aerosol-sat-Seoul run	Seoul	5500	Bin	500 m	Saturation adjustment	Bin-scheme sedimentation	Bin-scheme collection
Low-aerosol-sat-Seoul run	Seoul	550	Bin	500 m	Saturation adjustment	Bin-scheme sedimentation	Bin-scheme collection
High-aerosol-	Houston	1500	Bin	500 m	Saturation	Bin-scheme	Bin-scheme

sat-Houston run					adjustment	sedimentation	collection
Low-aerosol- sat-Houston run	Houston	150	Bin	500 m	Saturation adjustment	Bin-scheme sedimentation	Bin-scheme collection
High-aerosol- sed-Seoul run	Seoul	5500	Bin	500 m	Saturation adjustment	MG-scheme sedimentation	Bin-scheme collection
Low-aerosol- sed-Seoul run	Seoul	550	Bin	500 m	Saturation adjustment	MG-scheme sedimentation	Bin-scheme collection
High-aerosol- sed-Houston run	Houston	1500	Bin	500 m	Saturation adjustment	MG-scheme sedimentation	Bin-scheme collection
Low-aerosol- sed-Houston run	Houston	150	Bin	500 m	Saturation adjustment	MG-scheme sedimentation	Bin-scheme collection
High-aerosol- col-Seoul run	Seoul	5500	Bin	500 m	Saturation adjustment	MG-scheme sedimentation	MG-scheme collection
Low-aerosol- col-Seoul run	Seoul	550	Bin	500 m	Saturation adjustment	MG-scheme sedimentation	MG-scheme collection
High-aerosol- col-Houston run	Houston	1500	Bin	500 m	Saturation adjustment	MG-scheme sedimentation	MG-scheme collection
Low-aerosol- col-Houston run	Houston	150	Bin	500 m	Saturation adjustment	MG-scheme sedimentation	MG-scheme collection

FIGURE CAPTIONS

Figure 1. (a) Sea-level pressure (hPa) and (b) 850 hPa wind (m s^{-1} ; arrows), geopotential height (m; contours) and equivalent potential temperature (K; shaded) at 0900 LST July 26th 2011 over the northeast Asia. The rectangles in the Korean Peninsula in panels (a) and (b) mark the center of Seoul. (c) Sea-level pressure (hPa;shaded) and wind at 10 m above sea level (m s^{-1} ; barbs) and (d) convective available potential energy (J kg^{-1}) at 0500 LST 18 July 2013 in and around Houston. The rectangles in panels (c) and (d) mark the center of Houston.

Figure 2. (a) The domain (marked by the rectangle) used in simulations for the Seoul case. The small white circle marks the center of Seoul. (b) The domain used in simulations for the Houston case. The small white circle marks the center of Houston.

Figure 3. Vertical distributions of the time- and domain-averaged cloud liquid content (CLC) for (a) the Seoul case and (b) the Houston case. Solid lines represent simulations at the 500-m resolution, while dashed lines represent those at the 15-km resolution. Dotted lines represent simulations at the 35-km resolution and blue lines represent GFS-simulated CLC.

Figure 4. Same as Figure 3, but for cloud ice content (CIC).

1371 Figure 5. Time series of the domain-averaged (a) liquid water path (LWP) and (b) ice water path
1372 (IWP) for the Seoul case. Solid lines represent simulations at the 500-m resolution, while dashed and
1373 dotted lines represent those at 15- and 35-km resolutions, respectively. Blue lines represent GFS-
1374 simulated LWP and IWP and green lines represent observed LWP and IWP.

Deleted: km

1375
1376 Figure 6. Same as Figure 5, but for the Houston case.

1377
1378 Figure 7. Vertical distributions of the time- and domain-averaged updraft mass fluxes for (a) the Seoul
1379 case and (b) the Houston case. Solid lines represent simulations at the 500-m resolution, while dashed
1380 lines represent those at the 15-km resolution. Dotted lines represent simulations at the 35-km resolution
1381 and blue lines represent GFS-simulated updraft mass fluxes.

1382
1383 Figure 8. Vertical distributions of the time- and domain-averaged condensation rates for (a) the Seoul
1384 case and (b) the Houston case. Solid lines represent simulations at the 500-m resolution, while dashed
1385 lines represent those at the 15-km resolution. Dotted lines represent simulations at the 35-km resolution.

1386
1387 Figure 9. Same as Figure 8, but for deposition rates.

1388

1390 Figure 10. Distributions of normalized updraft frequency over updraft speeds for (a) the Seoul case
1391 and (b) the Houston case. Solid lines represent simulations at the 500-m resolution, while dashed lines
1392 represent those at the 15-km resolution. Dotted lines represent simulations at the 35-km resolution.

1393
1394 Figure 11. Same as Figure 8, but for evaporation rates.

1395
1396 Figure 12. Distributions of normalized precipitation frequency over precipitation rates for (a) the Seoul
1397 case and (b) the Houston case. Solid lines represent simulations at the 500-m resolution, while dashed
1398 lines represent those at the 15-km resolution. Dotted lines represent simulations at the 35-km resolution.

1399
1400 Figure 13. Vertical distributions of the time- and domain-averaged cloud liquid content (CLC) for (a)
1401 the Seoul case and (b) the Houston case. Solid red and black lines represent simulations with the bin
1402 scheme and at the 500-m resolution, while dashed red and black lines represent the bin-scheme
1403 simulations with the saturation adjustment. Solid yellow and green lines represent simulations with the
1404 MG scheme.

1405
1406 Figure 14. Vertical distributions of the time- and domain-averaged cloud liquid content (CLC) for (a)
1407 the Seoul case and (b) the Houston case. Solid red and black lines represent simulations with the bin
1408 scheme and at the 500-m resolution, while dashed red and black lines represent the bin-scheme

1409 simulations with the saturation adjustment and the MG scheme sedimentation process. Solid yellow
1410 and green lines represent simulations with the MG scheme.

1411

1412 Figure 15. Vertical distributions of the time- and domain-averaged cloud liquid content (CLC) for (a)
1413 the Seoul case and (b) the Houston case. Solid red and black lines represent simulations with the bin
1414 scheme and at the 500-m resolution, while dashed red and black lines represent the bin-scheme
1415 simulations with the saturation adjustment and the MG scheme sedimentation and collection processes.
1416 Solid yellow and green lines represent simulations with the MG scheme.

1417

1418

1419

1420

1421

1422

1423

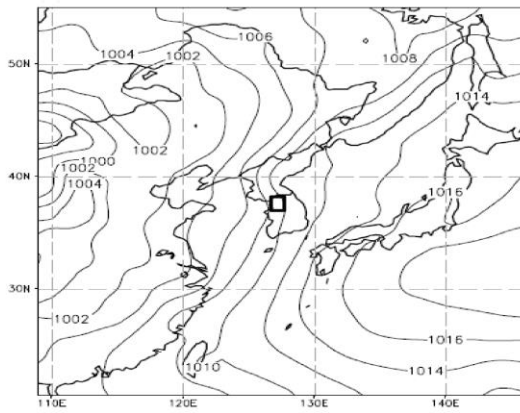
1424

1425

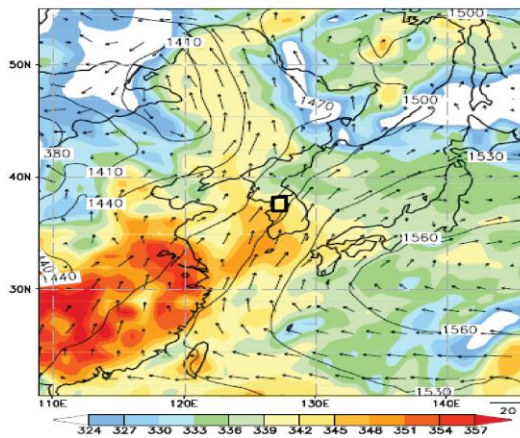
1426

1427

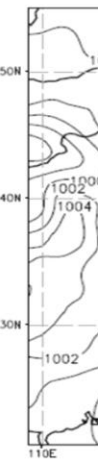
a



b



a



b

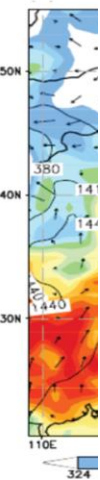


Figure 1

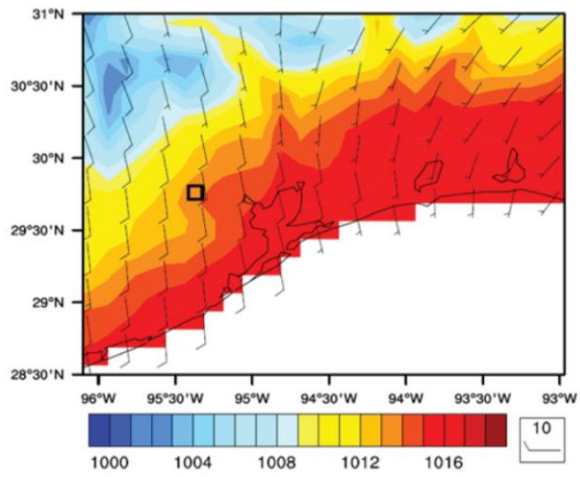
Deleted:
Deleted:

1428

1429

1430

c



d

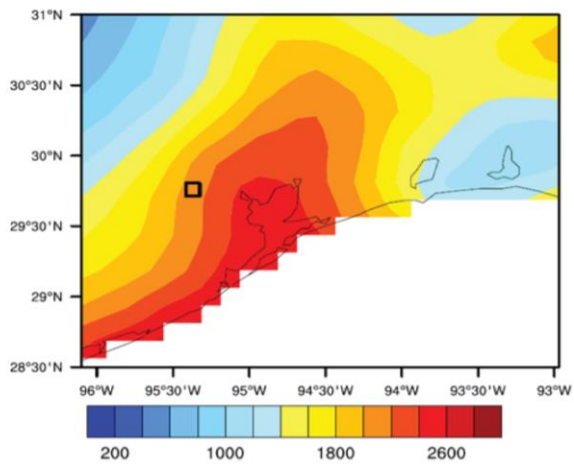
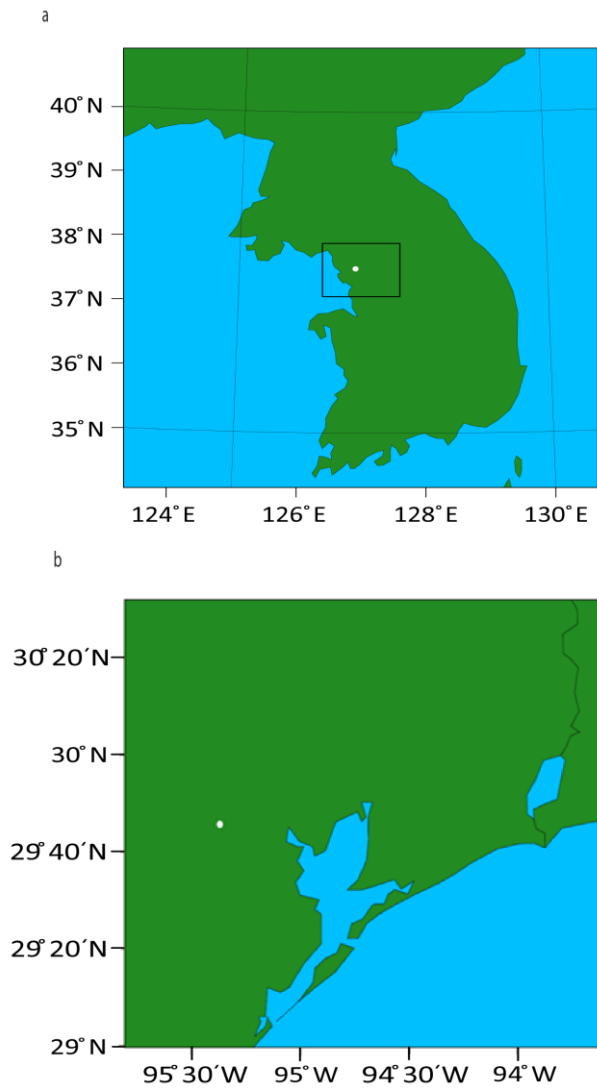
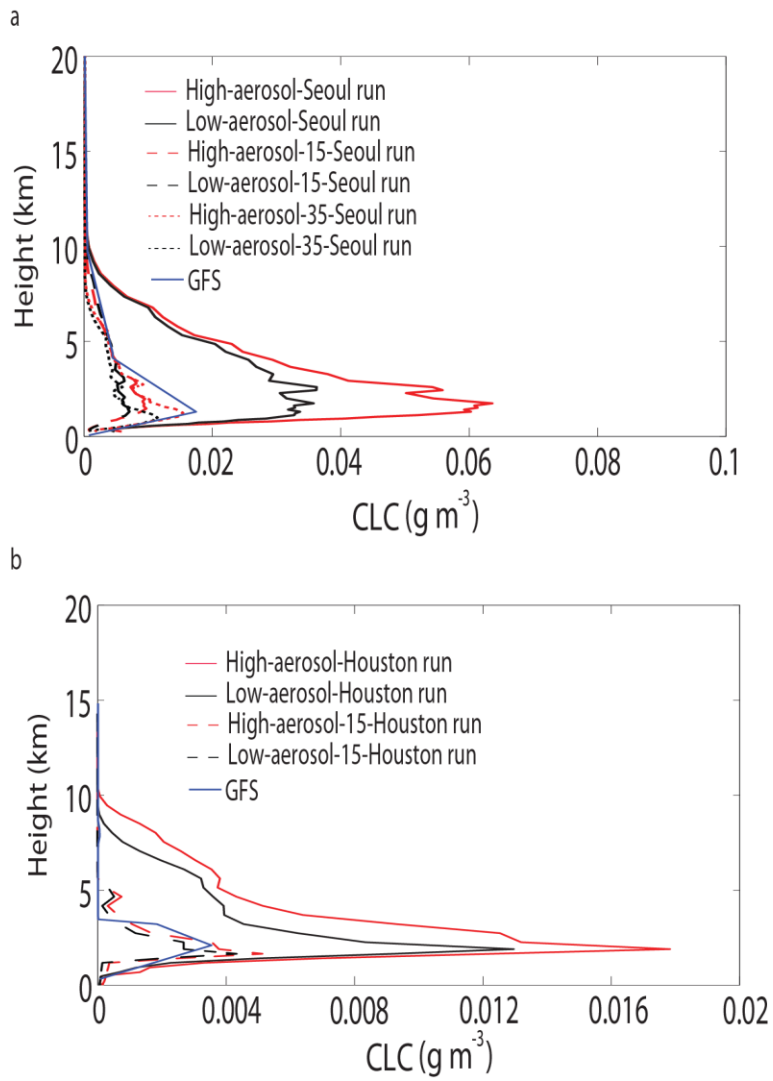


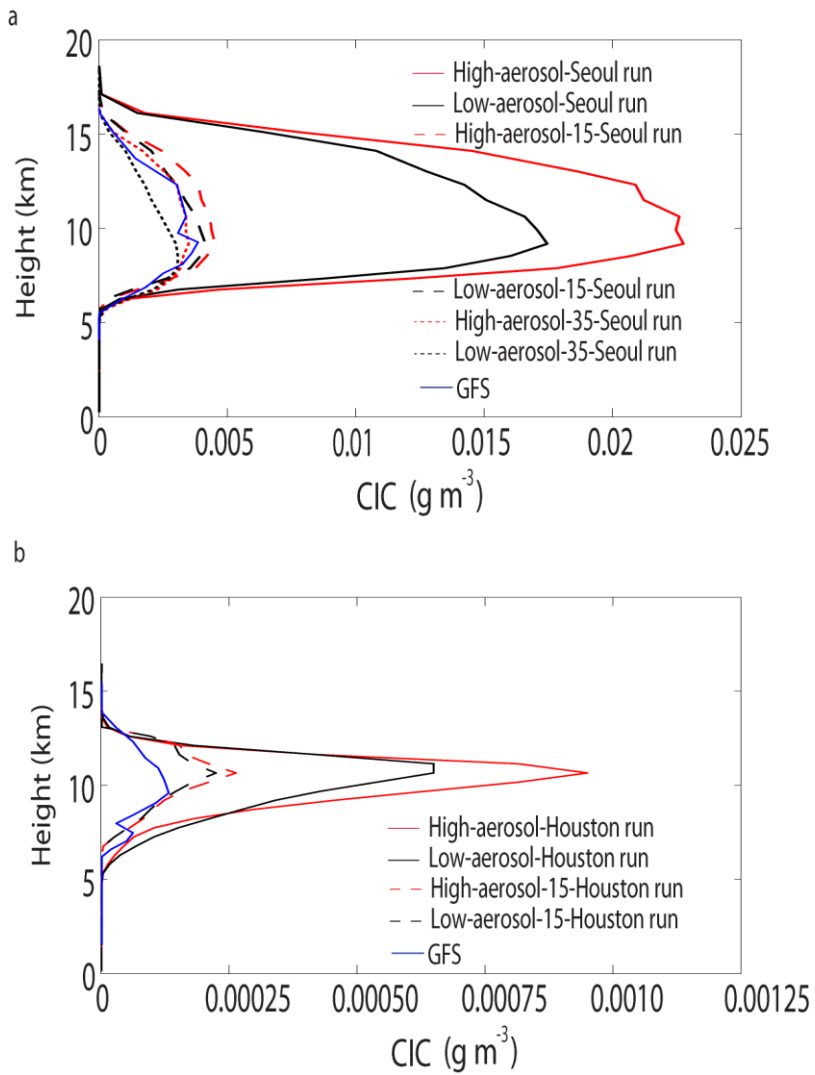
Figure 1

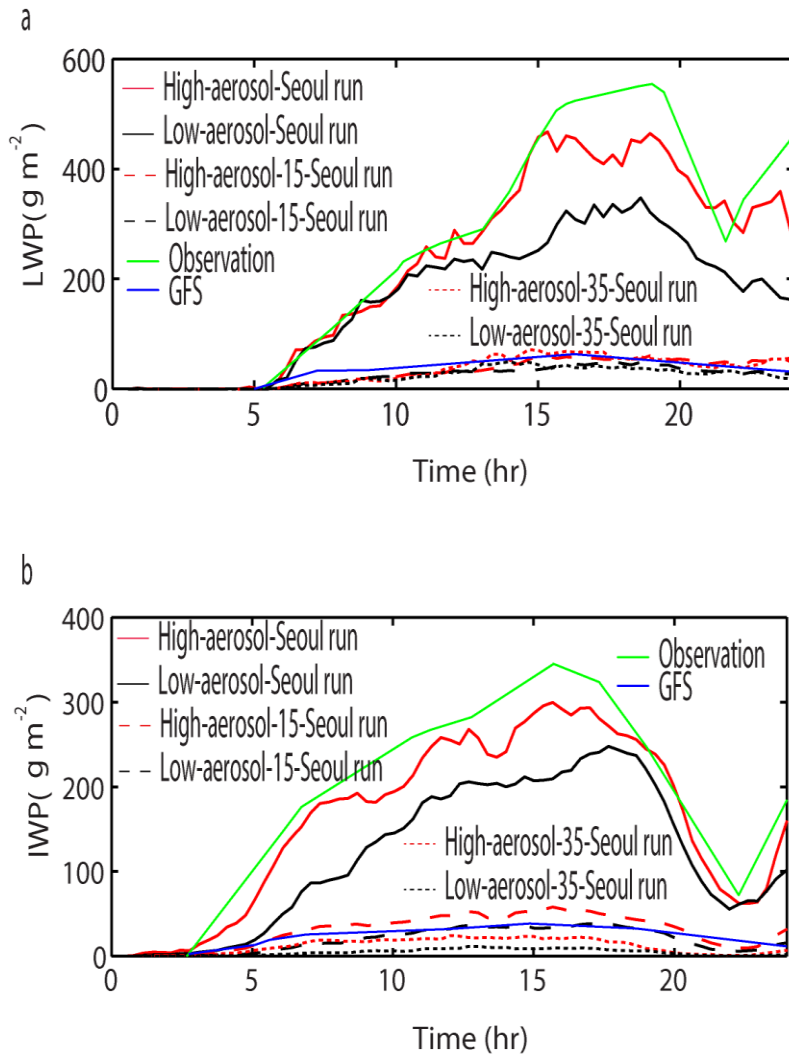
1433

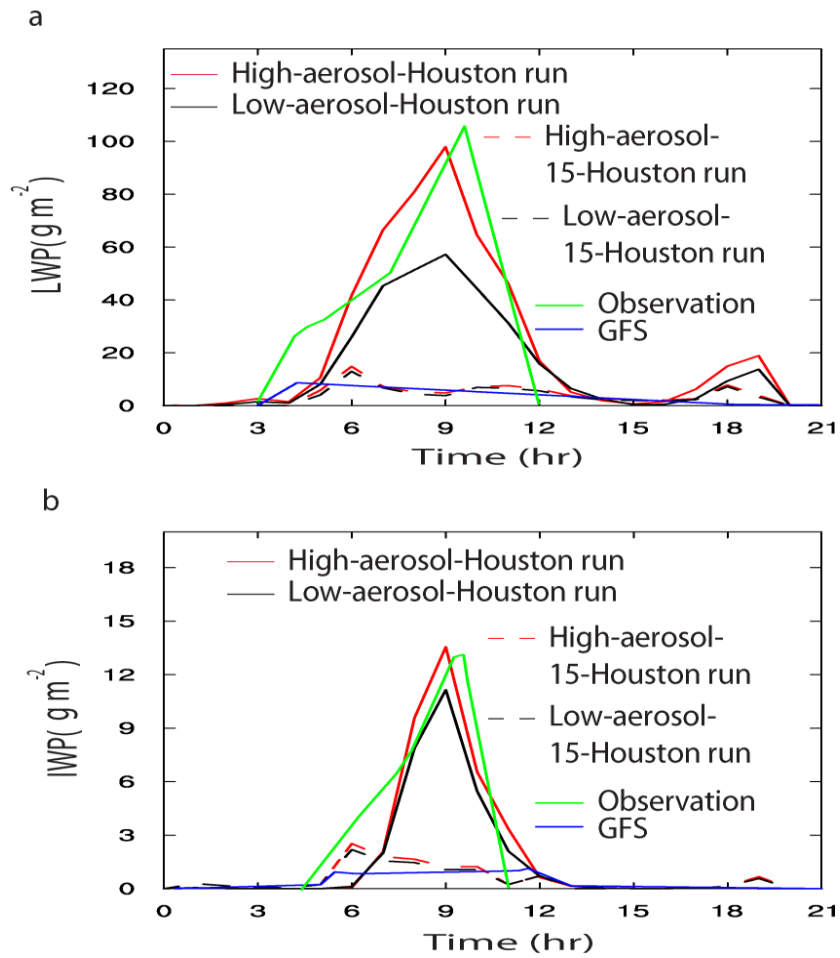
1434

**Figure 2**

**Figure 3**

**Figure 4**

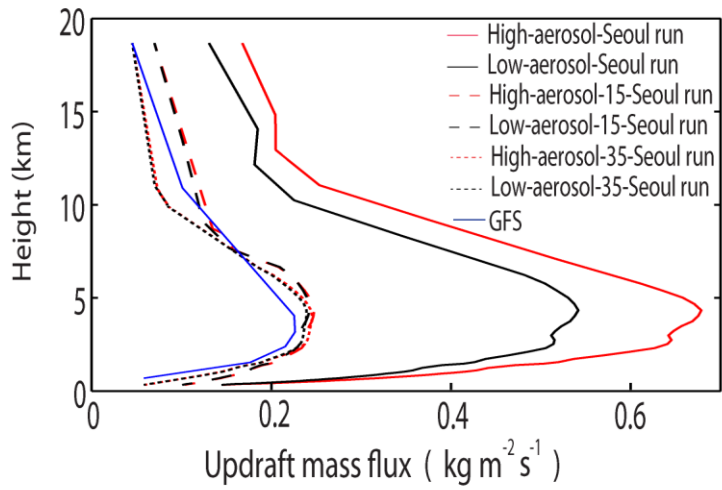
**Figure 5**

**Figure 6**

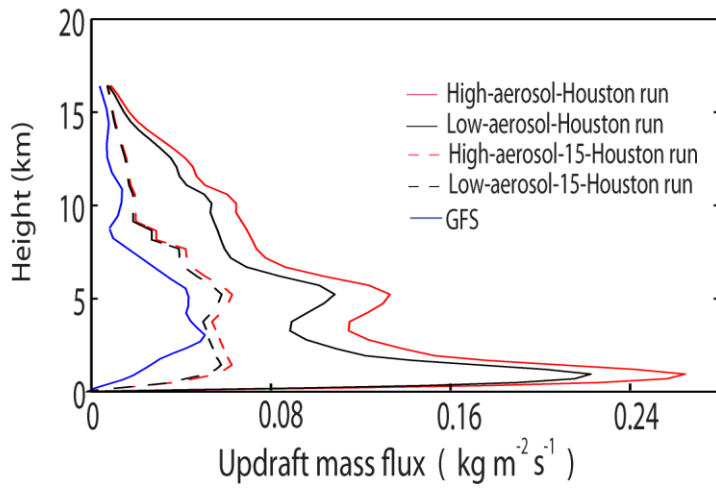
1443

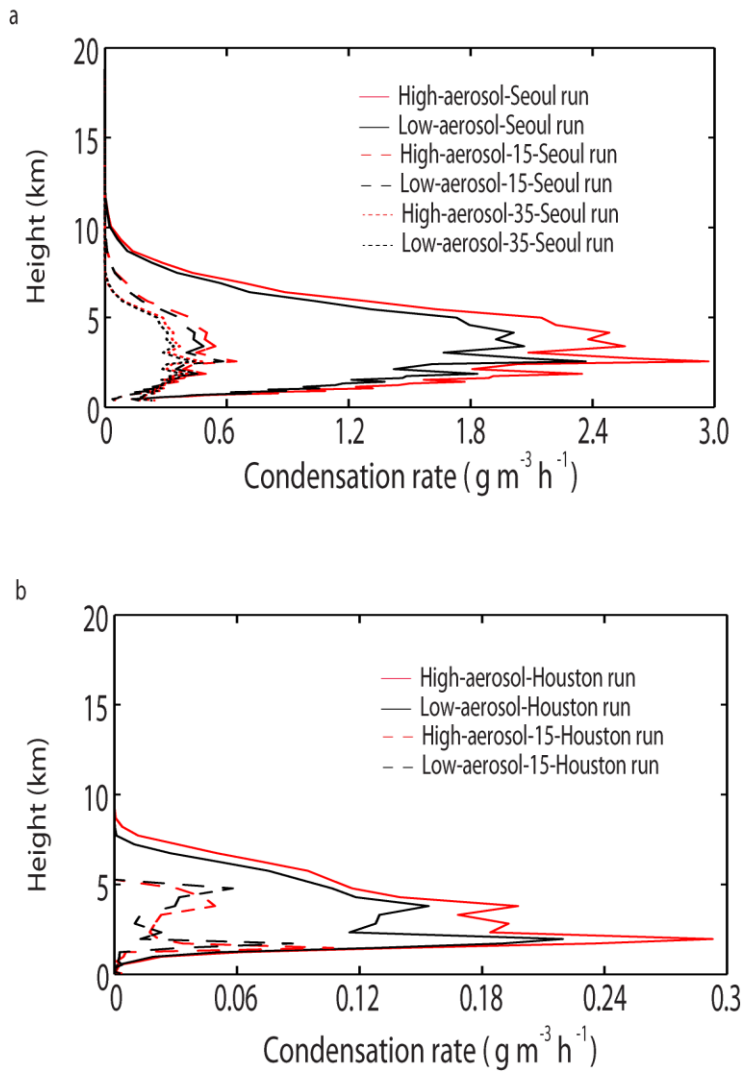
1444

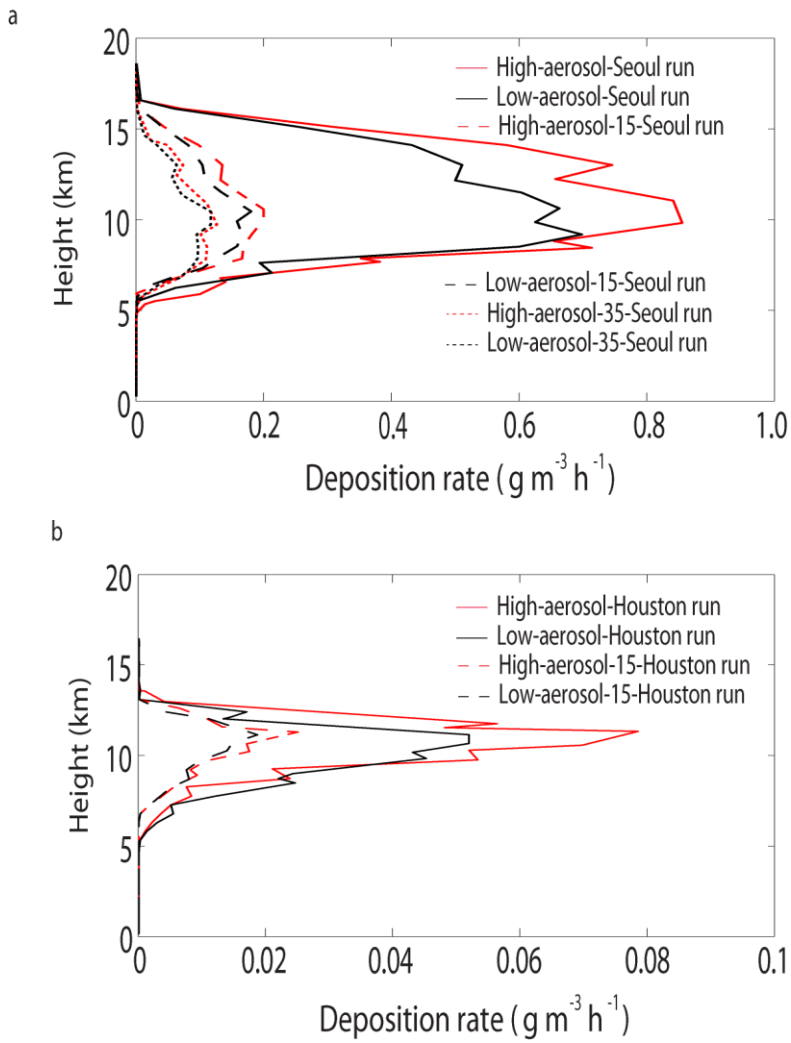
a

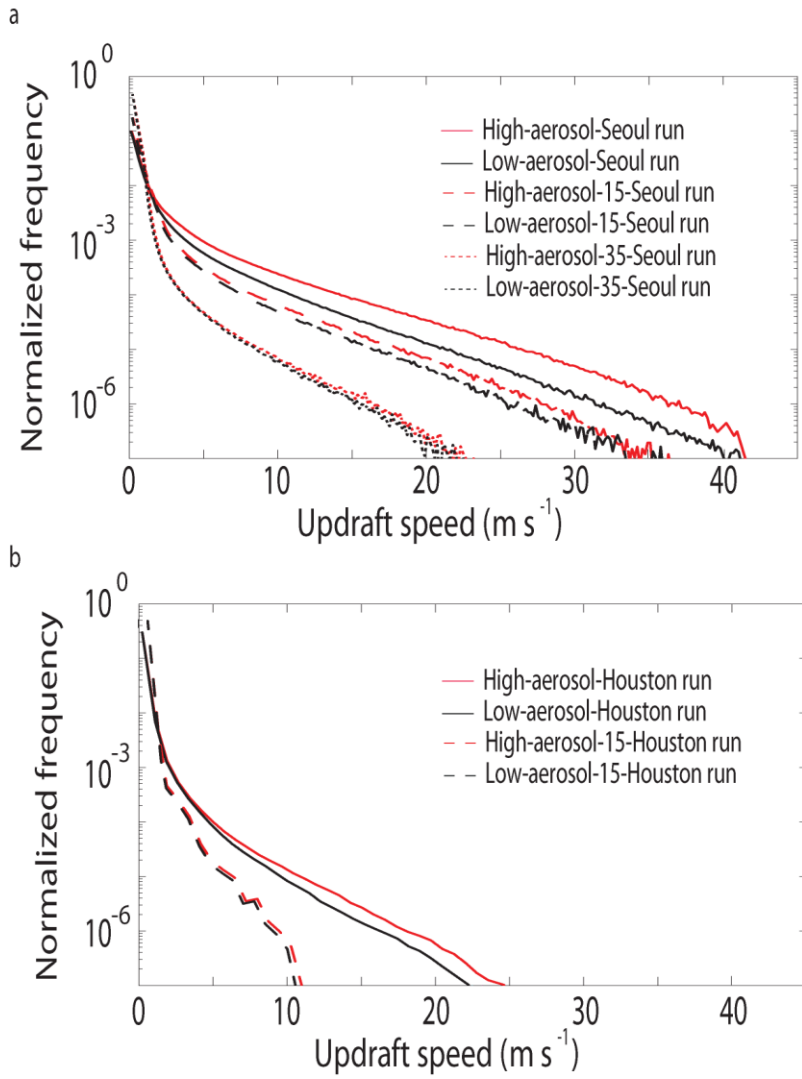


b

**Figure 7**

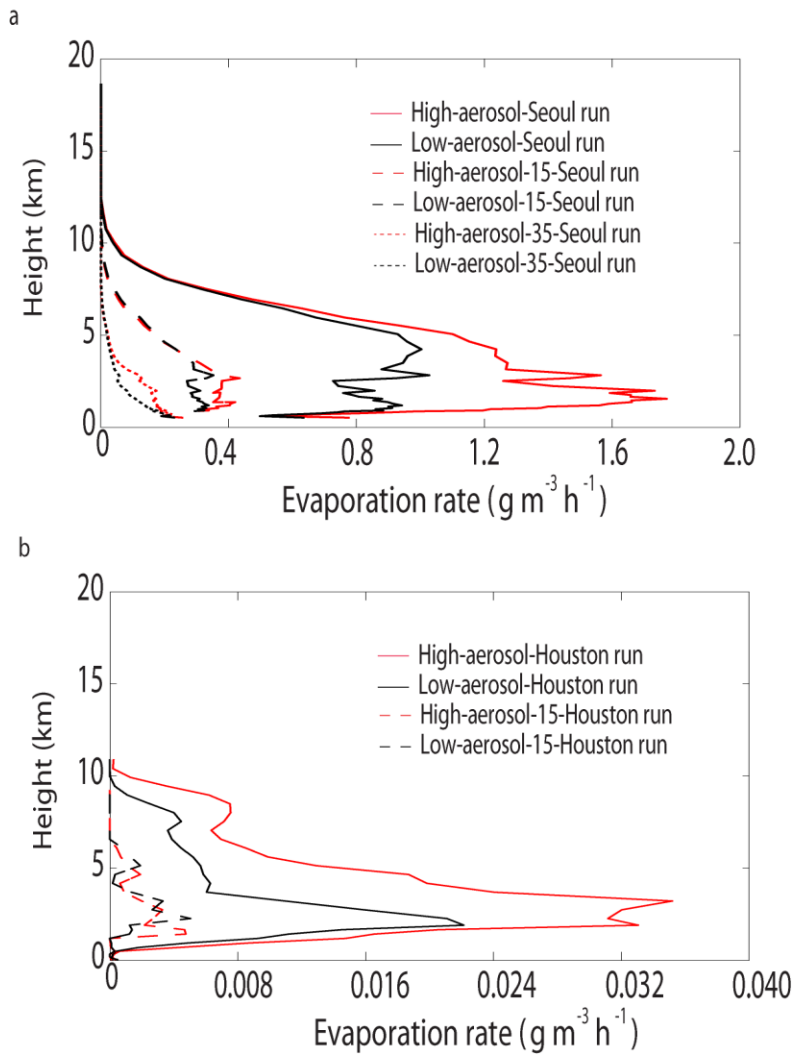
**Figure 8**

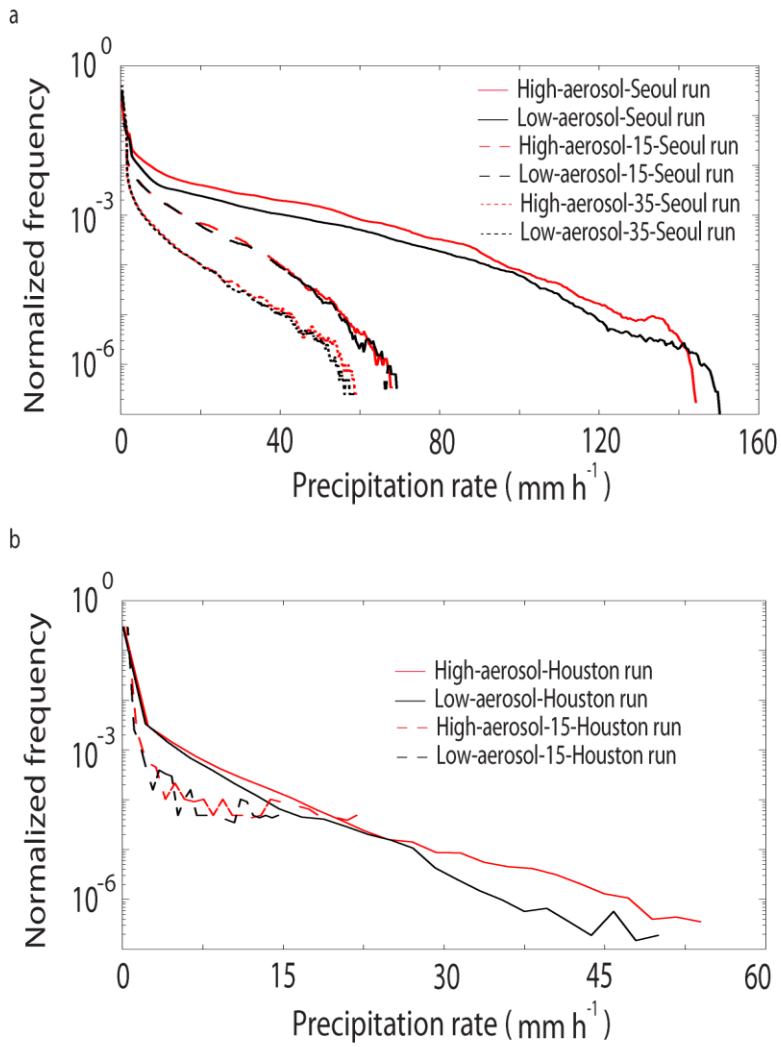
**Figure 9**

**Figure 10**

1451

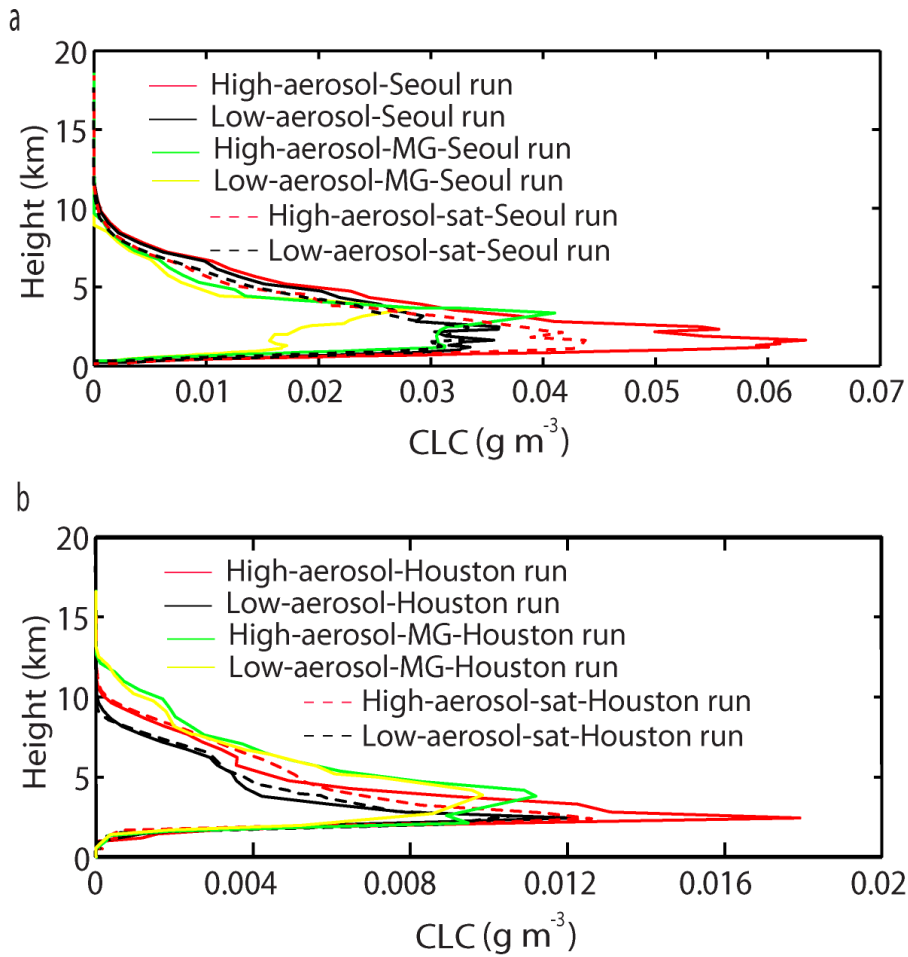
1452

**Figure 11**

**Figure 12**

1455

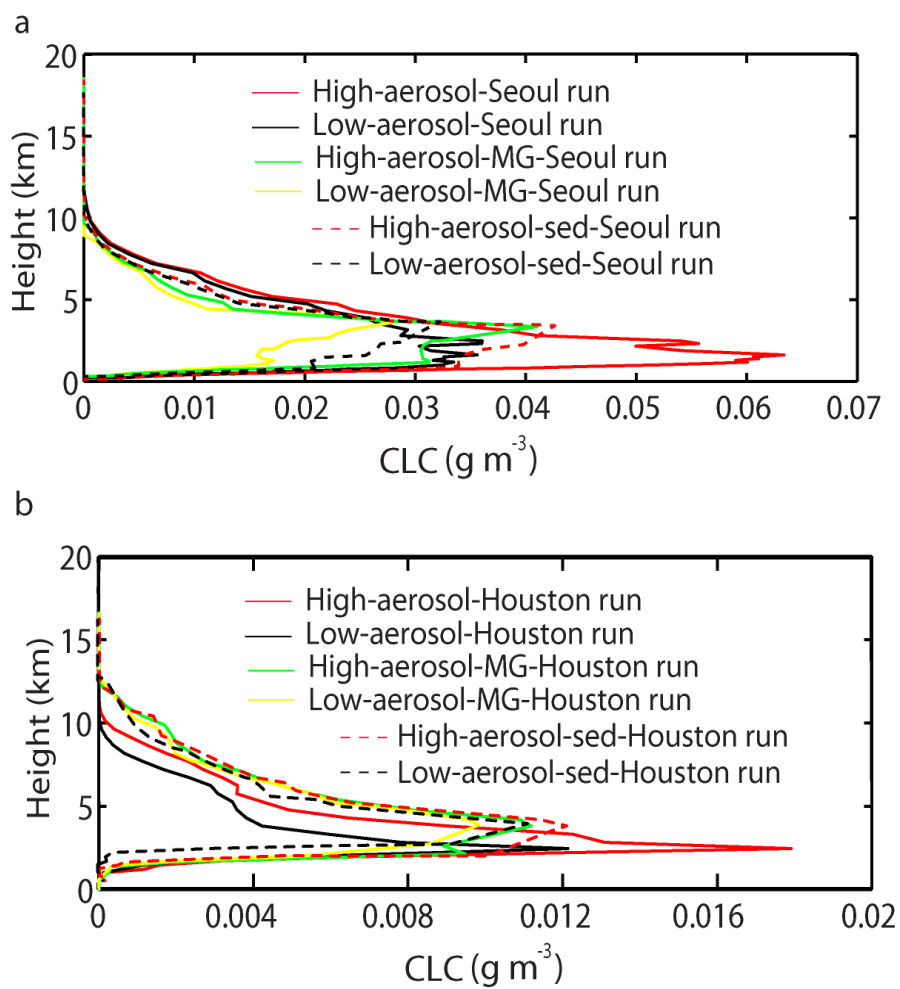
1456

**Figure 13**

1457

1458

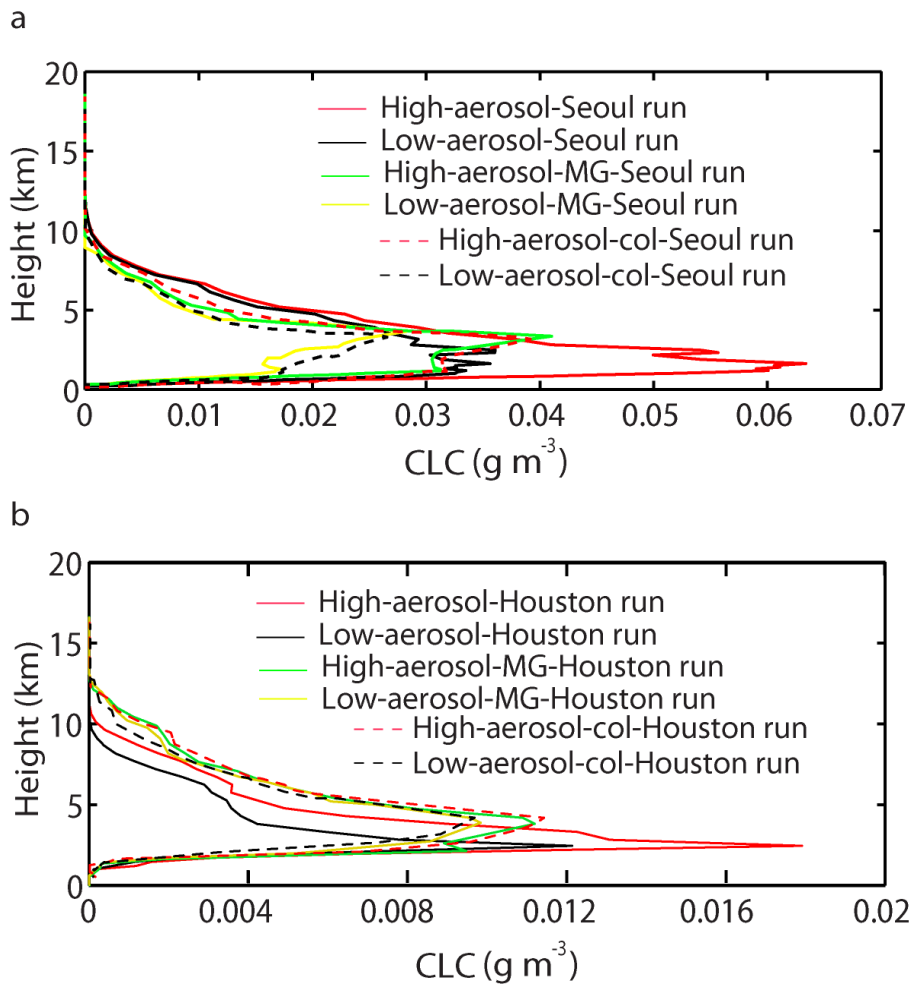
1459

**Figure 14**

1460

1461

1462

**Figure 15**

1463

1464

1465